

Twist-bend nematic phase from Landau-de Gennes perspective

Lech Longa^{ID}* and Wojciech Tomczyk^{ID}†

Jagiellonian University, Institute of Theoretical Physics,

Department of Statistical Physics, Łojasiewicza 11, 30-348 Kraków, Poland

(Dated: June 29, 2021)

Abstract

The understanding of self-organization in the twist-bend nematic (N_{TB}) phase, identified in 2011 in liquid crystal dimers, is at the forefront of soft matter research worldwide. This new nematic phase develops structural chirality in the isotropic (I) and the uniaxial nematic (N_{U}) phases, despite the fact that the molecules forming the structure are chemically *achiral*. Molecular, shape-induced flexopolarization provides a viable mechanism for a qualitative understanding of N_{TB} and the related phase transitions. The key question that remains is whether with this mechanism one can also explain quantitatively the presently existing experimental data. To address this issue we propose a generalization of the mesoscopic Landau-de Gennes theory of nematics, where higher-order elastic terms of the alignment tensor are taken into account, in addition to the lowest-order flexopolarization coupling. The theory is not only capable of explaining the appearance of N_{TB} but also stays in quantitative agreement with experimental data. In exemplary calculations, we take the data known for CB7CB flexible dimer - the “drosophila fly” in the studies of N_{TB} [A. Jákl et al., Rev. Mod. Phys. 90, 045004 (2018)] - and estimate the constitutive parameters of the model from temperature variation of the nematic order parameter and the Frank elastic constants in the nematic phase. Then we seek for relative stability and properties of the isotropic, uniaxial nematic and twist-bend nematic phases. In particular, we evaluate various properties of N_{TB} , like temperature variation of the structure’s wave vector, conical angle, flexopolarization, and remaining order parameters. We also look into the fine structure of N_{TB} , like its biaxiality - the property, which is difficult to access experimentally at the nanoscale.

* E-mail address: lech.longa@uj.edu.pl

† E-mail address: wojciech.tomczyk@doctoral.uj.edu.pl

I. INTRODUCTION

Undoubtedly, the short-pitch heliconical structure formed by an ensemble of achiral bent-core-like mesogens and commonly referred to as the nematic twist-bend, is one of the most astonishing liquid crystalline phases. It is the first example in nature of a structure where mirror symmetry is spontaneously broken without any support from a long-range positional order. The structure itself is a part of an over 130-year-old tradition of liquid crystal science demonstrating that even a minor change in the molecular chemistry can lead to a new type of liquid crystalline order, which differs in the degree of orientational and translational self-organization, ranging from molecular to macro scales [1–3].

The most common of all known liquid crystalline phases is the uniaxial nematic phase (N_U), where anisotropic molecules or molecular aggregates orient, on the average, parallel to each other. Their local, mean orientation at the point $\tilde{\mathbf{r}}$ of coordinates $(\tilde{x}, \tilde{y}, \tilde{z})$ is described by a single mesoscopic direction $\hat{\mathbf{n}}(\tilde{\mathbf{r}})$ ($|\hat{\mathbf{n}}(\tilde{\mathbf{r}})| = 1$), known as the director. Due to the statistical head-to-tail inversion symmetry of the local molecular arrangement the director states $\hat{\mathbf{n}}(\tilde{\mathbf{r}})$ and $-\hat{\mathbf{n}}(\tilde{\mathbf{r}})$ are equivalent. With an inversion symmetry and with a rotational symmetry of molecular orientational distribution about $\hat{\mathbf{n}}(\tilde{\mathbf{r}})$ the existence of the director is a basic property that distinguishes the uniaxial nematics from an ordinary isotropic liquid. That is, the N_U phase is a non-polar 3D liquid with long-range orientational order characterized by $\mathcal{D}_{\infty h}$ point group symmetry.

One important consequence of $\hat{\mathbf{n}}(\tilde{\mathbf{r}})$ being indistinguishable from $-\hat{\mathbf{n}}(\tilde{\mathbf{r}})$ is that the primary order parameter of the uniaxial nematics is the second-rank (3×3) traceless and symmetric alignment tensor (the quadrupole moment of the local angular distribution function of the molecules' long axes)

$$\tilde{\mathbf{Q}}_U(\tilde{\mathbf{r}}) = \tilde{S} \left(\hat{\mathbf{n}}(\tilde{\mathbf{r}}) \otimes \hat{\mathbf{n}}(\tilde{\mathbf{r}}) - \frac{1}{3} \mathbf{I} \right) \quad (1)$$

having components $\tilde{Q}_{U,\alpha\beta}$; \tilde{S} is the scalar order parameter describing the degree of (local) molecular orientational ordering along $\hat{\mathbf{n}}(\tilde{\mathbf{r}})$ and \mathbf{I} denotes the identity matrix.

Beyond conventional uniaxial nematics further nematic liquid phases, that (by definition) have only short-ranged positional ordering, were recognized. They involve \mathcal{D}_{2h} symmetric biaxial nematics (N_B) for non-chiral materials and cholesteric (N^*) along with blue phases (BP) for chemically chiral mesogens, characterized locally by \mathcal{D}_2 point group symmetry. In

order to account for their local orientational order we need a full, symmetric and traceless alignment tensor $\tilde{\mathbf{Q}}(\tilde{\mathbf{r}})$ with three different eigenvalues, as opposed to the uniaxial nematic (1), where only two eigenvalues of $\mathbf{Q} \equiv \mathbf{Q}_U$ are different.

This four-members nematic family is ubiquitous in nature and it has not been expanding for many years [1]. However, very recently the situation has changed with important discovery of two fundamentally new nematics: the twist-bend nematic phase (N_{TB}) [4–7] and the nematic splay phase (N_S) [8], and it seems these discoveries only mark a beginning of new, fascinating research direction in soft matter science [3, 9–12].

Without any doubt the discovered N_{TB} phase is different than 3D liquids known to date, because it exhibits a macroscopic chirality, while formed from chemically achiral, bent-core-like molecules. A direct manifestation of chirality is an average orientational molecular order that forms a local helix with a pitch spanning from several to over a dozen of nanometers, in the absence of any long-range positional order of molecular centers of mass. N_{TB} is stabilized as a result of (weakly) first order phase transition from the uniaxial nematic phase, or directly from the isotropic phase [13, 14] and therefore (as already mentioned) its emergence is probably one of the most unusual manifestation of mirror symmetry breaking (SMSB) in three-dimensional liquids.

At the theoretical level a possibility of SMSB in bent-shaped mesogens has been suggested by Meyer already in 1973. He pointed out that bend deformations, which should be favored by bent-shaped molecules, might lead to flexopolarization-induced chiral structures [15]. About thirty years later Dozov [16] considered the Oseen-Frank (OF) free energy $F_{OF} = \tilde{V}^{-1} \int_{\tilde{V}} f_{OF} d^3\tilde{\mathbf{r}}$ of the director field $\hat{\mathbf{n}}(\tilde{\mathbf{r}})$ [17, 18], where

$$f_{OF} = \frac{1}{2} [K_{11}(\tilde{\nabla} \cdot \hat{\mathbf{n}})^2 + K_{22}(\hat{\mathbf{n}} \cdot \tilde{\nabla} \times \hat{\mathbf{n}})^2 + K_{33}(\hat{\mathbf{n}} \times \tilde{\nabla} \times \hat{\mathbf{n}})^2], \quad (2)$$

and where K_{11} , K_{22} and K_{33} are splay, twist, and bend elastic constants, respectively. He correlated a possibility of SMSB in nematics with the sign change of the bend elastic constant, K_{33} . In this latter case, in order to guarantee the existence of a stable ground state, some higher order elastic terms had to be added to f_{OF} . Limiting to defect-free structures, Dozov predicted competition between a twist-bend nematic phase, where the director simultaneously twists and bends in space by precessing on the side of a right circular cone and a planar splay-bend phase with alternating domains of splay and bend, both shown in Fig. 1. If we take into account temperature dependence of the Frank elastic constants

then the uniaxial nematic phase becomes unstable to the formation of modulated structures at $K_{33} = 0$, which is the critical point of the model. The behaviour of the system depends on the relationship between the splay and twist elastic constants. As it turns out the twist-bend ordering wins if $K_{11} > 2K_{22}$, while the splay-bend phase is more stable if $K_{11} < 2K_{22}$. Assuming that the wave vector $\tilde{\mathbf{k}}$ of N_{TB} stays parallel to the $\hat{\mathbf{z}}$ -axis of the laboratory system of frame ($\tilde{\mathbf{k}} = \tilde{k}\hat{\mathbf{z}}$) the symmetry-dictated, gross features of the heliconical N_{TB} structure are essentially accounted for by the uniform director modulation

$$\hat{\mathbf{n}}(\tilde{z}) = \mathcal{R}_{\hat{\mathbf{z}}}(\phi)\hat{\mathbf{n}}(0) = [\cos(\phi)\sin(\theta), \sin(\phi)\sin(\theta), \cos(\theta)], \quad (3)$$

where $\hat{\mathbf{n}}(0) = [\sin(\theta), 0, \cos(\theta)]$ and where $\mathcal{R}_{\hat{\mathbf{z}}}(\phi) = \mathcal{R}_{\hat{\mathbf{z}}}(\phi(\tilde{z}))$ is the homogeneous rotation about $\hat{\mathbf{z}}$ through the azimuthal angle $\phi = \pm\tilde{k}\tilde{z} = \pm 2\pi\tilde{z}/p$ and where p is the pitch. The \pm sign indicates that both left-handed and right-handed chiral domains should form with the same probability, which is manifestation of SMSB in the bulk. Note that the molecules in N_{TB} are inclined, on the average, from $\tilde{\mathbf{k}}$ by the conical angle θ – the angle between $\hat{\mathbf{n}}$ and the wave vector $\tilde{\mathbf{k}}$ (Fig. 1). The symmetry of N_{TB} also implies that the structure must be locally polar with the polarization vector, $\tilde{\mathbf{P}}$, staying perpendicular both to the director and the wave vector

$$\tilde{\mathbf{P}}(\tilde{z}) = \mathcal{R}_{\hat{\mathbf{z}}}(\phi)\tilde{\mathbf{P}}(0) = \tilde{p}_0 [\sin(\phi), -\cos(\phi), 0]. \quad (4)$$

Hence, in the nematic twist-bend phase, both $\hat{\mathbf{n}}$ and $\tilde{\mathbf{P}}$ rotate along the helix direction $\tilde{\mathbf{k}}$ giving rise to a phase with constant bend and twist deformation of no mass density modulation (Fig. 1).

In 2013 Shamid *et al.* [19] developed a Landau theory for bend flexoelectricity and showed that the results of Dozov are in line with Meyer’s idea of flexopolarization-induced N_{TB} . Their theory predicts a continuous $N - N_{\text{TB}}$ transition, where the effective bend elastic constant, renormalized by the flexopolarization coupling, changes sign for sufficiently large coupling. The corresponding structure develops modulated polar order, averaging to zero globally as in Eq. (4). The Dozov’s model is also supported by measurements of anomalously small bend elastic constant (compared to the splay and twist elastic constants) in the nematic phase of materials exhibiting N_{TB} (*see e.g.* measurements for CB7CB dimer of Babakhanova *et al.* [20–22]).

The second most widely used continuum model to characterize orientational properties of nematics is the minimal coupling, $SO(3)$ -symmetric Landau-de Gennes (LdeG) expansion

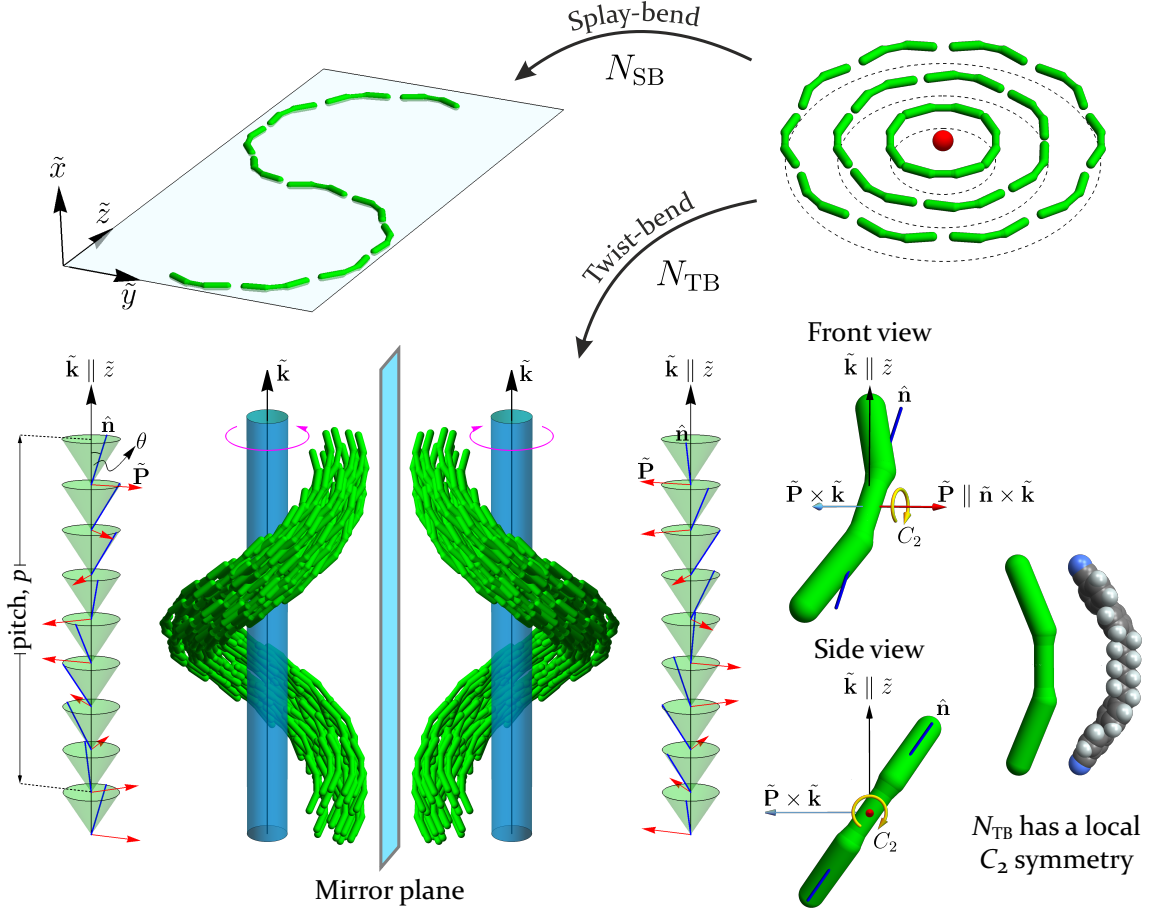


FIG. 1. Pure bend distortion in 2D leads to the emergence of defects (red sphere). Their appearance can be circumvented by alternating the bend direction periodically or allowing nonzero twist by lifting bend into the third dimension. These possibilities, respectively, give rise to the two alternative nematic ground states: splay-bend (N_{SB}) and twist-bend (N_{TB}). Twist-bend nematic has been firstly observed in the phase sequence of liquid crystal dimer, 1'',7''-bis(4-cyanobiphenyl-4'-yl)heptane (CB7CB), where two identical cyanobiphenyl mesogenic groups are linked by a heptane spacer (CB7CB molecule can be viewed as having three parts: two identical rigid end groups connected by a flexible spacer). Schematic representation of molecular organization in the N_{TB} with right and left handedness (ambidextrous chirality) has been depicted at the bottom of the image. Right/left circular cone of conical angle θ shows the tilt between the director \hat{n} and the helical symmetry axis, parallel to the wave vector \tilde{k} . Red arrow represents polarization \tilde{P} , where $\tilde{P} \parallel \tilde{k} \times \hat{n}$; black arrow is the direction of \tilde{k} . Note that N_{TB} has a local C_2 symmetry with a two-fold symmetry axis around \tilde{P} .

in terms of the local alignment tensor. It allows not only to account for a fine structure of inhomogeneous nematic phases, but also shows important generalizations of the director's description in dealing with orientational degrees of freedom (*see e.g.* [23]). In a series of papers [11, 12, 24], co-authored by one of us, we developed an extension of the LdeG theory to include flexopolarization couplings. The extended theory predicted that the flexopolarization mechanism can make the N_{TB} phase absolutely stable within the whole family of one-dimensional modulated structures [11]. A qualitatively correct account of experimental observations in N_{TB} (*see e.g.* [3]) was obtained, like trends in temperature variation of the helical pitch and conical angle, and behaviour in the external electric field [25]. The theory also predicted weakly first order phase transitions from the isotropic and nematic to the nematic twist-bend phase, again in agreement with experiments [14, 26]. Despite this qualitative success of the LdeG modelling one important theoretical issue still left unsolved is that associated with the elastic behaviour of the uniaxial nematic phase for materials with stable N_{TB} . A few existing measurements of all three elastic constants in the N_{U} phase show that $K_{11} \gtrsim 2K_{22}$ ($K_{22} \approx 3 - 4$ pN), while $K_{33} \approx 0.4$ pN near the transition into N_{TB} [20]. That is, the splay elastic constant is about 20 times larger than the bend elastic constant. On the theoretical side, the LdeG expansion with only two distinct bulk elastic terms cannot explain this anomalously large disparity in the values of K_{11} and K_{33} . Actually, it predicts that they both are equal in the Oseen-Frank limit [27, 28], where the alignment tensor is given by Eq. (1). Therefore, there are anomalously small bend and splay Frank elastic constants on approaching N_{TB} in the LdeG model with flexopolarization [12]. Though this prediction might suggest a dominance of the structures with splay-bend deformations over the twist-bend ones, the N_{TB} phase, as already discussed before, can still be found to be more stable than any of one-dimensional periodic structures, including the nematic splay-bend phase [11]. Most probably this is due to the remarkable (and unique) feature of N_{TB} of being uniform everywhere in space that makes the $SO(3)$ -symmetric elastic free energy density independent of space variables [11].

Central to quantitative understanding of N_{TB} and related phase transitions is then a construction of a generalized LdeG theory that releases the $K_{11} = K_{33}$ restriction of the minimal coupling model and accounts for the experimental behaviour of the Frank elastic constants in the vicinity of $N_{\text{U}} - N_{\text{TB}}$ phase transition. We expect that such a theory will allow for a systematic study of mesoscopic mechanisms that can be responsible for chiral

symmetry breaking in nematics. It will also give a new insight into conditions that can potentially lead experimentalists to a discovery of new nematic phases. Although the choice of strategy has already been worked out in the literature [24, 29, 30] the main problem lies in a huge number of elastic invariants in the alignment tensor, contributing to the generalized elastic free energy density of nematics. Here we show how the problem can be solved in a systematic way if we start from a theory which holds without limitations for arbitrary one-dimensional periodic distortions of the alignment tensor. These distortions form the most interesting class of structures for it obeys the recently discovered new nematic phases. An additional requirement for the generalized LdeG theory is that its ground state in the absence of flexopolarization should be that corresponding to a constant tensor field $\tilde{\mathbf{Q}}$. The theory so constructed will then be applied to characterize properties of N_{TB} formed in the class of CB7CB-like dimers and its constitutive parameters will be estimated from experimental data known for the CB7CB dimers in the N_{U} phase.

This paper is organized as follows. In Section II a tensor representation for N_{TB} and classification of all homogeneously deformed nematic phases is introduced. In Sections III and IV a generalized Landau-de Gennes theory is developed for nematic structures that are periodic only in one spatial direction. In Section V bifurcation scenarios to homogeneously deformed nematics are given. In Sections VI and VII the theory is confronted with experimental data for CB7CB. In particular, some estimates of constitutive parameters of the theory are found from the data for CB7CB in the N_{U} phase. Then the theory is used to study properties of N_{TB} along with an extensive comparison of the results with available experimental data. Predictions are also given for the order parameters and the degree of biaxiality of N_{TB} . The paper is concluded with final remarks in Section VIII.

II. ALIGNMENT TENSOR REPRESENTATION FOR HOMOGENEOUSLY DEFORMED NEMATIC PHASES

In the N_{TB} phase the director $\hat{\mathbf{n}}$ and the polarization vector $\tilde{\mathbf{P}}$ are given by Eqs. (3) and (4), while the equivalent alignment tensor order parameter, $\tilde{\mathbf{Q}}_{U,\text{TB}}$, is obtained by substituting (3) into (1). Though these models seem to account for gross features of orientational order observed in N_{TB} they do not exhaust possible nematic structures that can fill space with twist, bend and splay. A full spectrum of possibilities is obtained by studying an ex-

pansion of the biaxial alignment tensor $\tilde{\mathbf{Q}}$ and the polarization field $\tilde{\mathbf{P}}$ in spin tensor modes of $L = 2$ and $L = 1$, respectively, and in plane waves [12]. Within this huge family of states an important class of nematic structures is represented by uniformly deformed states (UDS) where the elastic, $SO(3)$ -symmetric invariants contributing to the elastic free energy density of nematics [24, 30] are constant in space. For such structures the same tensor and polarization landscape is seen everywhere in space. They are periodic in, at most, one spatial direction, say \tilde{z} , and fill uniformly space without defects. In analogy to the conditions (3) and (4) for $\hat{\mathbf{n}}$ and \mathbf{P} , they are generated from the tensors $\tilde{\mathbf{Q}}(0)$ and $\tilde{\mathbf{P}}(0)$ for $\tilde{z} = 0$ by the previously defined homogeneous rotation $\mathcal{R}_{\tilde{z}}(\pm\tilde{k}\tilde{z}) \equiv \mathcal{R}_{\tilde{z}}(\phi)$ [11, 31]. More specifically

$$\begin{aligned}\mathcal{R}_{\tilde{z}}(\pm\tilde{k}\tilde{z})\tilde{\mathbf{Q}}(0) &= \tilde{\mathbf{Q}}(\tilde{z}), \\ \mathcal{R}_{\tilde{z}}(\pm\tilde{k}\tilde{z})\tilde{\mathbf{P}}(0) &= \tilde{\mathbf{P}}(\tilde{z}),\end{aligned}\tag{5}$$

where \pm labels left- (+) and right-handed (-) heliconical structures. Hence, the most general representations for UDS that generalizes Eqs. (3) and (4), can be cast in the form [11, 31]:

$$\tilde{\mathbf{Q}}(\tilde{z}) = \frac{\tilde{x}_0}{\sqrt{6}} \begin{bmatrix} -1 & 0 & 0 \\ 0 & -1 & 0 \\ 0 & 0 & 2 \end{bmatrix} + \frac{\tilde{r}_{\pm 1}}{\sqrt{2}} \begin{bmatrix} 0 & 0 & -c_{\pm 1} \\ 0 & 0 & s_{\pm 1} \\ -c_{\pm 1} & s_{\pm 1} & 0 \end{bmatrix} + \frac{\tilde{r}_{\pm 2}}{\sqrt{2}} \begin{bmatrix} c_{\pm 2} & -s_{\pm 2} & 0 \\ -s_{\pm 2} & -c_{\pm 2} & 0 \\ 0 & 0 & 0 \end{bmatrix},\tag{6}$$

$$\tilde{\mathbf{P}}(\tilde{z}) = \tilde{p}_{\pm 1} \begin{bmatrix} -\cos(\pm\tilde{k}\tilde{z} + \phi_{\pm p}) \\ \sin(\pm\tilde{k}\tilde{z} + \phi_{\pm p}) \\ 0 \end{bmatrix} + \tilde{v}_0 \begin{bmatrix} 0 \\ 0 \\ 1 \end{bmatrix},\tag{7}$$

where $c_{\pm m} = \cos(\pm m\tilde{k}\tilde{z} + \phi_{\pm m})$ and $s_{\pm m} = \sin(\pm m\tilde{k}\tilde{z} + \phi_{\pm m})$ and where nine real parameters \tilde{x}_0 , $\pm\tilde{k}$, $\tilde{r}_{\pm i} \geq 0$, $\tilde{p}_{\pm 1} \geq 0$, \tilde{v}_0 , $\phi_{\pm m}$ and $\phi_{\pm p}$ for each of the \pm labels characterize the fine structure of the phases, especially its biaxiality. Indeed, an arbitrary symmetric and traceless tensor field $\tilde{\mathbf{Q}}$ fulfills the inequalities (*see discussion in* [32]):

$$-1 \leq w = \frac{\sqrt{6} \text{Tr}(\tilde{\mathbf{Q}}^3)}{\text{Tr}(\tilde{\mathbf{Q}}^2)^{\frac{3}{2}}} \leq 1,\tag{8}$$

which are satisfied as equalities for locally prolate ($w = 1$) and oblate ($w = -1$) uniaxial phases. States of nonzero biaxiality are realized for $-1 < w < 1$, with maximal biaxiality

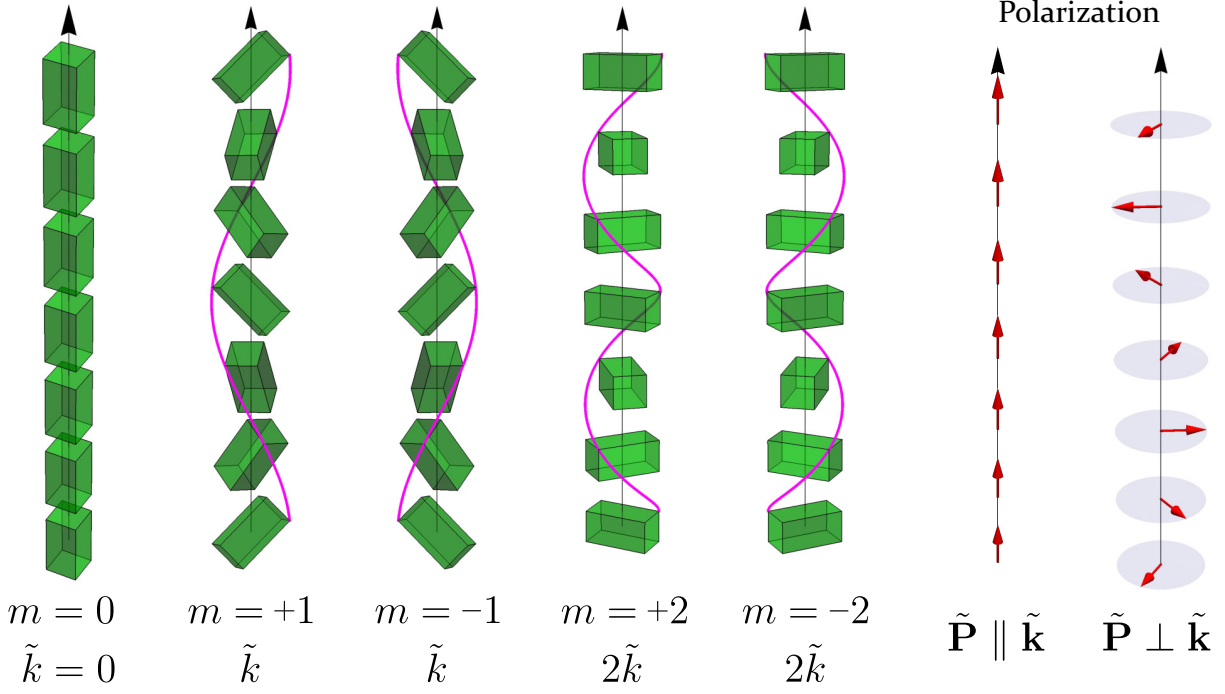


FIG. 2. Visualization of helicity modes: $m = 0$, $m = \pm 1$ and $m = \pm 2$ (change of m into $-m$ corresponds to replacement of $\tilde{\mathbf{k}}$ by $-\tilde{\mathbf{k}}$). Bricks represent the tensor $\tilde{\mathbf{Q}}(\tilde{\mathbf{r}})$ where the eigenvectors of $\tilde{\mathbf{Q}}(\tilde{\mathbf{r}})$ are parallel to their arms, while the absolute values of eigenvalues are their lengths. Red arrows represent the polarization field $\tilde{\mathbf{P}}(\tilde{\mathbf{r}})$.

corresponding to $w = 0$. In particular, the parameter $w(\tilde{\mathbf{Q}}(\tilde{z}))$ for $\tilde{\mathbf{Q}}(\tilde{z})$ given by Eq. (6) reads

$$w(\tilde{\mathbf{Q}}(\tilde{z})) = \frac{\frac{3}{2}\tilde{r}_{\pm 1}^2 (\sqrt{3}\tilde{r}_{\pm 2} \cos(2\phi_{\pm 1} - \phi_{\pm 2}) + \tilde{x}_0) - 3\tilde{r}_{\pm 2}^2 \tilde{x}_0 + \tilde{x}_0^3}{(\tilde{r}_{\pm 1}^2 + \tilde{r}_{\pm 2}^2 + \tilde{x}_0^2)^{3/2}}. \quad (9)$$

Note that in agreement with definition (5), the parameter $w(\tilde{\mathbf{Q}}(\tilde{z}))$ is position-independent and can take arbitrary value within the allowed $[-1, 1]$ interval, Eq. (8). In contrast, for the uniaxial tensor $\tilde{\mathbf{Q}}_{U,TB}$, corresponding to $\tilde{x}_0 = \frac{\sqrt{6}S}{12}(1 + 3\cos(2\theta))$, $\tilde{r}_{\pm 1} = \frac{\sqrt{2}S}{2}\sin(2\theta)$ and $\tilde{r}_{\pm 2} = \frac{\sqrt{2}S}{2}\sin(\theta)^2$ the parameter $w(\tilde{\mathbf{Q}}_{U,TB}) = \text{Sign}(S) = \pm 1$ (θ is the conical angle).

We should mention that the fields in Eqs. (6) and (7) are insensitive to choice of the origin of the laboratory system of frame, which allows to eliminate one of the phases $\phi_{\pm i}$ ($i = 1, 2, p$), independently for each of the two states with “+” and “-” subscripts. The coefficients in Eqs. (6) and (7) are chosen such that the norms squared of the order parameters are sums of squares of the coefficients: $\text{Tr}(\tilde{\mathbf{Q}}^2) = \tilde{x}_0^2 + \tilde{r}_{\pm 1}^2 + \tilde{r}_{\pm 2}^2$ and $\text{Tr}(\tilde{\mathbf{P}}^2) = \tilde{p}_{\pm 1}^2 + \tilde{v}_0^2$. Together, $\tilde{\mathbf{Q}}$ and $\tilde{\mathbf{P}}$ characterize a family of all defect-free homogeneously distorted (polar) helical/heliconical

TABLE I. Family of uniformly deformed nematic structures that can be constructed out of the fields $\tilde{\mathbf{Q}}$ and $\tilde{\mathbf{P}}$. Limiting cases of constant $\tilde{\mathbf{Q}}$ and $\tilde{\mathbf{P}}$ are also included.

Structure	Nonzero amplitudes	Abbreviation
Nonpolar structures		
(a) uniaxial nematic	\tilde{x}_0	N_U
(b) biaxial nematic	$\tilde{x}_0, \tilde{r}_1, \tilde{r}_2, \tilde{k} \rightarrow 0$	N_B
(c) (ambidextrous) cholesteric	$\tilde{x}_0, \tilde{r}_2, \tilde{k}_{N^*} = 2\tilde{k} \neq 0$	N_C
Locally polar structures		
(d) locally polar cholesteric	as in (c), \tilde{p}_1	N_{Cl}
(e) nematic twist-bend	$\tilde{x}_0, \tilde{r}_1, \tilde{r}_2, \tilde{p}_1, \tilde{k} \neq 0$	N_{TB}
Globally polar structures		
(f) polar (a)–(e)	any of (a)–(e), \tilde{v}_0	add subscript “ p ” to (a)–(e)

nematic phases (they are gathered in Table I).

III. GENERALIZED LANDAU-DE GENNES EXPANSION FOR 1D PERIODIC NEMATICS

In this section we introduce a generalized Landau-de Gennes free energy (GLdeG) expansion in $\tilde{\mathbf{Q}}$ and $\tilde{\mathbf{P}}$ capable of quantitative description of the systems with stable one-dimensional periodic nematics. The most important members of this family are the nematic twist-bend phase [3] and recently discovered nematic splay phase [8]. Our main effort in this and next section will concentrate on general characterization of GLdeG. An example

of spatially homogeneous structures with its prominent representative - the N_{TB} phase - will be studied in great detail. Parameters entering the LdeG expansion will be estimated from experimental data for the CB7CB compound in the uniaxial nematic phase. Then, the properties of the N_{TB} phase resulting from so constructed GLdeG expansion will be calculated and compared with available experimental data.

We assume that the stabilization of N_{TB} is due to entropic, excluded volume flexopolarization interactions [33], induced by sterically polar molecular bent cores. The direct interactions between electrostatic dipoles will be disregarded [33] and long-range polar order will be attributed to the molecular shape polarity. With $\tilde{\mathbf{Q}}$ and $\tilde{\mathbf{P}}$ the general LdeG expansion then reads [24, 28]

$$\tilde{F} = \frac{1}{\tilde{V}} \int_{\tilde{V}} \tilde{f}_{\text{tot}} d^3\tilde{\mathbf{r}} = \frac{1}{\tilde{V}} \int_{\tilde{V}} \left(\tilde{f}_{b,Q} + \tilde{f}_{e,Q} + \tilde{f}_P + \tilde{f}_{QP} \right) d^3\tilde{\mathbf{r}}, \quad (10)$$

where $\tilde{\mathbf{r}}$ is the position vector, \tilde{V} is the system's volume and where the free energy densities, $\tilde{f}_{x,X}$, \tilde{f}_X , are constructed out of the fields X . They involve the bulk nematic part $\tilde{f}_{b,Q}$, the nematic elastic part $\tilde{f}_{e,Q}$ and the parts \tilde{f}_P and \tilde{f}_{QP} responsible for the onset of chirality in the nematic phase. Although the general theory has plenty of constitutive parameters part of them, at least for CB7CB, can be estimated from existing experimental data for the N_U and at the $I - N_U$ and $N_U - N_{\text{TB}}$ phase transitions. One of the issues we would like to understand is whether the theory so constructed allows to account for the quantitative properties of the nematic twist-bend phase, below $N_U - N_{\text{TB}}$ phase transition.

A. Bulk nematic free energy

According to the phenomenological Landau-de Gennes (LdG) theory the equilibrium bulk properties of nematics can be found from a nonequilibrium free energy, constructed as an $SO(3)$ -symmetric expansion in powers of $\tilde{\mathbf{Q}}$. There are only two types of independent $SO(3)$ invariants that can be constructed out of $\tilde{\mathbf{Q}}$, namely $\text{Tr}(\tilde{\mathbf{Q}}^2)$ and $\text{Tr}(\tilde{\mathbf{Q}}^3)$. Hence \tilde{f}_{Qb} is a polynomial in $\text{Tr}(\tilde{\mathbf{Q}}^2)$ and $\text{Tr}(\tilde{\mathbf{Q}}^3)$ with the only restriction on the expansion being that it must be stable against an unlimited growth of $\tilde{\mathbf{Q}}$. As we will show the experimental data for \tilde{S} in the nematic phase of CB7CB fit well to a model where the expansion with respect to $\tilde{\mathbf{Q}}$ is taken at least up to sixth order terms. More specifically, in the absence of electric and magnetic fields, introducing $\tilde{I}_2 = \text{Tr}(\tilde{\mathbf{Q}}^2)$ and $\tilde{I}_3 = \text{Tr}(\tilde{\mathbf{Q}}^3)$, we take for the bulk free

energy density of the isotropic and the nematic phases

$$\tilde{f}_{Qb} = \tilde{f}_{Qb}[\tilde{I}_2, \tilde{I}_3] = a_Q \tilde{I}_2 - b \tilde{I}_3 + c \tilde{I}_2^2 + d \tilde{I}_2 \tilde{I}_3 + e \left(\tilde{I}_2^3 - 6 \tilde{I}_3^2 \right) + f \tilde{I}_3^2. \quad (11)$$

A full account of phases, critical and tricritical points that this theory predicts is found in [32].

The coefficients of the expansion (11) generally depend on temperature and other thermodynamic variables, but in Landau theory the explicit temperature dependence is retained only in the bulk part, quadratic in $\tilde{\mathbf{Q}}$. In what follows, as a measure of temperature we choose the relative temperature distance, Δt , from the nematic-isotropic phase transition, defined through the relation

$$a_Q = a_{0Q} \frac{(T - T^*)}{T_{NI}} = a_{0Q} \left(\frac{T - T_{NI}}{T_{NI}} + \frac{T_{NI} - T^*}{T_{NI}} \right) = a_{0Q} (\Delta t + \Delta t_{NI}), \quad (12)$$

where $a_{0Q} > 0$, T is the absolute temperature, T_{NI} is the nematic-isotropic transition temperature, T^* is the spinodal for a first-order phase transition from the isotropic phase to the uniaxial nematic phase, $\Delta t = (T - T_{NI})/T_{NI} \leq 0$ and $\Delta t_{NI} = (T_{NI} - T^*)/T_{NI} > 0$ is the reduced temperature distance of nematic-isotropic transition temperature from T^* . Additionally, $b, c, d, e > 0$ and $f > 0$ are the temperature independent expansion coefficients. The last two conditions for e and f guarantees that \tilde{f}_{Qb} is stable against an unlimited growth of $\tilde{\mathbf{Q}}$ [32]. The expansion, Eq. (11), generally accounts for the isotropic, uniaxial nematic and biaxial nematic phases [32, 34].

We should mention that the fourth order expansion, where $c > 0$ and $d = e = f = 0$ predicts that the N_{TB} phase can be absolutely stable within the family of one-dimensional modulated structures [11], but the theory does not give a quantitative agreement with the data for \tilde{S} in the nematic phase of CB7CB unless unphysically large value of Δt_{NI} is taken.

B. Elastic free energy

A spatial deformation of the alignment tensor $\tilde{\mathbf{Q}}$ in the nematic phase is measured by the elastic free energy density \tilde{f}_{Qel} of the Landau free energy expansion (10). For the description of elastic properties of nematic liquid crystals \tilde{f}_{Qel} usually is expanded into powers of $\tilde{\mathbf{Q}}$ and its first derivatives $\partial \tilde{\mathbf{Q}} \equiv \partial \tilde{Q}_{ij} / \partial \tilde{x}_k = \tilde{Q}_{ij,k}$, where only quadratic terms in derivatives of the order parameter field are retained, in line with similar expansion for the director field, Eq. (2).

This standard, the so called minimal-coupling Landau-de Gennes expansion for \tilde{f}_{Qel} , comprises of only two elastic terms: $[L_1^{(2)}] = \tilde{Q}_{\alpha\beta,\gamma}\tilde{Q}_{\alpha\beta,\gamma}$ and $[L_2^{(2)}] = \tilde{Q}_{\alpha\beta,\beta}\tilde{Q}_{\alpha\gamma,\gamma}$. Although again the theory, Eq. (10), with \tilde{f}_{Qel} containing only these two elastic terms accounts for absolutely stable N_{TB} among one-dimensional modulated structures [11] it is not sufficiently general to quantitatively reproduce, *e.g.* elastic properties of bent-core systems in the parent nematic phase for it implies equality of splay and bend Frank elastic constants, which so far is not an experimentally supported scenario with stable N_{TB} . Thus, we need to include higher-order elastic terms in the LdeG theory to account for experimentally observed elastic behaviour of bent-core mesogens. A general form of the LdeG elastic free energy density has been studied by Longa *et al.* in a series of papers [24, 28, 30]. As it turns out the most important are third-order invariants of the form $\tilde{\mathbf{Q}}\partial\tilde{\mathbf{Q}}\partial\tilde{\mathbf{Q}}$, given explicitly in Supplemental Material, because they are the lowest order terms removing splay-bend degeneracy of the second-order theory [28]. But with quadratic and cubic terms alone the elastic free energy \tilde{f}_{Qel} is unbounded from below and, hence, cannot represent a correct theory of nematics. To assure the nematic ground state is stable against an unlimited growth of $\tilde{Q}_{\alpha\beta}$ and $\tilde{Q}_{\alpha\beta,\gamma}$ we need to add some fourth-order invariants [28]. In total, there are 22 deformation modes $[L_i^{(n)}]$ of $\tilde{\mathbf{Q}}$ up to the order $\tilde{\mathbf{Q}}\tilde{\mathbf{Q}}\partial\tilde{\mathbf{Q}}\partial\tilde{\mathbf{Q}}$ (*see* Supplemental Material for details). The next step is to single out the relevant elastic terms $[L_i^{(n)}]$ that should enter the expansion \tilde{f}_{Qel} . A considerable reduction in the number of independent terms is obtained if we limit ourselves to a class of one-dimensional periodic structures $\tilde{\mathbf{Q}}(\tilde{z} + \tilde{p}) = \tilde{\mathbf{Q}}(\tilde{z})$ [11, 35]. Then, the only relevant linearly independent $[L]$ -terms are

- $\partial\tilde{\mathbf{Q}}\partial\tilde{\mathbf{Q}}$ terms: $[L_1^{(2)}], [L_2^{(2)}]$
- $\tilde{\mathbf{Q}}\partial\tilde{\mathbf{Q}}\partial\tilde{\mathbf{Q}}$ terms: $[L_2^{(3)}], [L_3^{(3)}], [L_4^{(3)}]$
- $\tilde{\mathbf{Q}}\tilde{\mathbf{Q}}\partial\tilde{\mathbf{Q}}\partial\tilde{\mathbf{Q}}$ terms: $[L_2^{(4)}], [L_3^{(4)}], [L_5^{(4)}], [L_6^{(4)}], [L_7^{(4)}], [L_{10}^{(4)}], [L_{11}^{(4)}]$.

As mentioned before the most important are third order terms $\tilde{\mathbf{Q}}\partial\tilde{\mathbf{Q}}\partial\tilde{\mathbf{Q}}$ linear in $\tilde{\mathbf{Q}}$ and quadratic in $\partial\tilde{\mathbf{Q}}$, because they remove splay-bend degeneracy [28]. Hence, in what follows we will keep the third-order terms and add three stabilizing terms of the order $\tilde{\mathbf{Q}}\tilde{\mathbf{Q}}\partial\tilde{\mathbf{Q}}\partial\tilde{\mathbf{Q}}$. More specifically, for the elastic free energy \tilde{f}_{Qel} we take a sum of quadratic terms in deformations

of the form:

$$\begin{aligned} \tilde{f}_{Qel} &= L_1^{(2)} \tilde{Q}_{\alpha\beta,\gamma} \tilde{Q}_{\alpha\beta,\gamma} + L_2^{(2)} \tilde{Q}_{\alpha\beta,\beta} \tilde{Q}_{\alpha\gamma,\gamma} + L_{14}^{(4)} \left(\lambda_2 \tilde{Q}_{\mu\nu,\nu} + \tilde{Q}_{\alpha\beta} \tilde{Q}_{\alpha\mu,\beta} \right)^2 + \\ &\quad L_6^{(4)} \left(\lambda_3 \tilde{Q}_{\beta\nu,\nu} + \tilde{Q}_{\alpha\beta} \tilde{Q}_{\alpha\mu,\mu} \right)^2 + L_7^{(4)} \left(\lambda_4 \tilde{Q}_{\beta\mu,\nu} + \tilde{Q}_{\alpha\beta} \tilde{Q}_{\alpha\mu,\nu} \right)^2 \end{aligned} \quad (13)$$

$$\begin{aligned} &= \left(L_1^{(2)} + \lambda_4^2 L_7^{(4)} \right) \left[L_1^{(2)} \right] + \left(L_2^{(2)} + \lambda_2^2 L_{14}^{(4)} + \lambda_3^2 L_6^{(4)} \right) \left[L_2^{(2)} \right] + \\ &\quad L_2^{(3)} \left[L_2^{(3)} \right] + L_{14}^{(4)} \left[L_{14}^{(4)} \right] + L_3^{(3)} \left[L_3^{(3)} \right] + L_6^{(4)} \left[L_6^{(4)} \right] + L_4^{(3)} \left[L_4^{(3)} \right] + L_7^{(4)} \left[L_7^{(4)} \right] \end{aligned} \quad (14)$$

where the coefficients $L_i^{(n)}$ denote temperature-independent elastic constants that couple with the invariant $\left[L_i^{(n)} \right]$ and where $\lambda_2 = L_2^{(3)} / \left(2L_{14}^{(4)} \right)$, $\lambda_3 = L_3^{(3)} / \left(2L_6^{(4)} \right)$, and $\lambda_4 = L_4^{(3)} / \left(2L_7^{(4)} \right)$. Use of the $\left[L_{14}^{(4)} \right]$ invariant, which is a linear combination of the invariants $\tilde{\mathbf{Q}}\tilde{\mathbf{Q}}\partial\tilde{\mathbf{Q}}\partial\tilde{\mathbf{Q}}$, allows to write the stability criteria for \tilde{f}_{Qel} in a simple form (see Supplemental Material). Indeed, the elastic free energy density \tilde{f}_{Qel} is a sum of positive-definite terms if

$$\begin{aligned} L_1^{(2)} &> 0, \quad L_1^{(2)} + \frac{2}{3}L_2^{(2)} > 0, \\ L_6^{(4)} &> 0 \quad \vee \quad L_6^{(4)} = 0 \wedge L_3^{(3)} = 0, \\ L_7^{(4)} &> 0 \quad \vee \quad L_7^{(4)} = 0 \wedge L_4^{(3)} = 0, \\ L_{14}^{(4)} &> 0 \quad \vee \quad L_{14}^{(4)} = 0 \wedge L_2^{(3)} = 0. \end{aligned} \quad (15)$$

The conditions (15) are sufficient ones for \tilde{f}_{Qel} to be positive definite ($\tilde{f}_{Qel} \geq 0$). For smooth tensor fields $\tilde{\mathbf{Q}}$ the ground state of \tilde{f}_{Qel} ($\tilde{f}_{Qel} = 0$) corresponds to a constant, position-independent $\tilde{\mathbf{Q}}$, which represents an unperturbed uniaxial or biaxial nematic state. As we show in section VI the elastic constants $L_m^{(n)}$ entering expansion (14) can all be estimated from the data for Frank elastic constants in the uniaxial nematic phase. To conclude, the free energy (14) is a thermodynamically stable expansion of the Landau-de Gennes free energy in the local alignment tensor, complete up to third-order for deformations realized in one spatial direction.

The elastic free energy (14) can still be written in a simpler form by further selecting terms that are relevant for UDS. Indeed, substitution of Eq. (6) into expansion (14) induces extra relations between cubic and quartic elastic invariants, namely

$$\left[L_2^{(3)} \right] = -2 \left[L_3^{(3)} \right], \quad \left[L_{14}^{(4)} \right] = 4 \left[L_6^{(4)} \right]. \quad (16)$$

Thus, in seeking for a relative stability of UDS two elastic terms in (14) are still redundant. This redundancy becomes especially transparent in the parameterization where the elastic

constants $L_2^{(3)}$, $L_3^{(3)}$, $L_6^{(4)}$ and $L_{14}^{(4)}$ are replaced by appropriate linear combinations of $L_7^{(3)}$, $L_8^{(3)}$, $L_{15}^{(4)}$ and $L_{16}^{(4)}$. They are given by

$$\begin{aligned} L_2^{(3)} &= L_8^{(3)} - L_7^{(3)}, & L_3^{(3)} &= 2 \left(L_8^{(3)} + L_7^{(3)} \right), \\ L_6^{(4)} &= 4 \left(L_{15}^{(4)} - L_{16}^{(4)} \right), & L_{14}^{(4)} &= L_{15}^{(4)} + L_{16}^{(4)}. \end{aligned} \quad (17)$$

where, in addition, the inequality $L_{15}^{(4)} > \left| L_{16}^{(4)} \right|$ is required to fulfill stability conditions (15). Substitution of (17) into (14) now yields

$$\begin{aligned} \tilde{f}_{Qel} &= \left(L_1^{(2)} + \lambda_4^2 L_7^{(4)} \right) \left[L_1^{(2)} \right] + \left(L_2^{(2)} + \lambda_2^2 L_{14}^{(4)} + \lambda_3^2 L_6^{(4)} \right) \left[L_2^{(2)} \right] + \\ &L_7^{(3)} \left[L_7^{(3)} \right] + L_{15}^{(4)} \left[L_{15}^{(4)} \right] + L_8^{(3)} \left[L_8^{(3)} \right] + L_{16}^{(4)} \left[L_{16}^{(4)} \right] + L_4^{(3)} \left[L_4^{(3)} \right] + L_7^{(4)} \left[L_7^{(4)} \right], \end{aligned} \quad (18)$$

where

$$\begin{aligned} \left[L_7^{(3)} \right] &= 2 \left[L_3^{(3)} \right] - \left[L_2^{(3)} \right], \\ \left[L_8^{(3)} \right] &= 2 \left[L_3^{(3)} \right] + \left[L_2^{(3)} \right], \\ \left[L_{15}^{(4)} \right] &= \left[L_{14}^{(4)} \right] + 4 \left[L_6^{(4)} \right], \\ \left[L_{16}^{(4)} \right] &= \left[L_{14}^{(4)} \right] - 4 \left[L_6^{(4)} \right], \end{aligned} \quad (19)$$

and where $\left[L_8^{(3)} \right]$ and $\left[L_{16}^{(4)} \right]$ terms vanish for UDS, given by Eq. (6).

C. Coupling with steric polarization

According to the current understanding of the formation of stable twist–bend nematic phase its orientational order, being similar to that of smectic C^* [1], should be accompanied with a long-range polar order of molecular bent cores [36–40]. As already pointed out the other direct molecular interactions, such as between electrostatic dipoles, are probably less relevant for thermal stability of this phase. Up to the leading order in $\tilde{\mathbf{P}}$ at least five extra terms must be included in \tilde{f}_P and \tilde{f}_{QP} , Eq. (10). They read [11, 12, 28]

$$\tilde{f}_P = a_P \tilde{\mathbf{P}}^2 + A_4 (\tilde{\mathbf{P}}^2)^2 + b_P (\tilde{\nabla} \otimes \tilde{\mathbf{P}})^2, \quad (20)$$

$$\tilde{f}_{QP} = -\varepsilon_P \tilde{\mathbf{P}} \cdot (\tilde{\nabla} \cdot \tilde{\mathbf{Q}}) - \Lambda_{QP} \tilde{P}_\alpha \tilde{Q}_{\alpha\beta} \tilde{P}_\beta. \quad (21)$$

Here $a_P = a_{0P}((T - T_P)/T_{NI}) = a_{0P}(\Delta t + \Delta t_{NI,P})$, where $\Delta t_{NI,P} = (T_{NI} - T_P)/T_{NI} > 0$, $A_4 > 0$, $b_P > 0$, ε_P and Λ_{QP} are further temperature-independent constitutive parameters of

the model. Again, limitations for A_4 and b_P stem from stability requirement of a ground state against unlimited fluctuations of $\tilde{\mathbf{P}}(\tilde{\mathbf{r}})$. The ε_P -term represents lowest-order flexopolarization contribution while the Λ_{QP} -term is the direct coupling between the polarization field and the alignment tensor. The presently existing experimental data seem in line with this minimal coupling expansion for the (flexo)polarization part of the free energy [11, 12]. A full structure of the (flexo)polarization theory, along with some of its general consequences, can be found in [24].

IV. REDUCED FORM OF GENERALIZED LANDAU DE-GENNES EXPANSION

For practical calculations it is useful to reduce the number of model parameters by rewriting Eq. (10) in terms of reduced (dimensionless) quantities. It reveals the redundancy of four parameters in the expressions (11,14,20,21) and allows to set them to one from the start [12, 24, 28, 29]. This reduction is a direct consequence of the freedom to choose a scale for the free energy, $\tilde{F} = \Lambda_F F$, for the fields $\tilde{\mathbf{Q}} = \Lambda_Q \mathbf{Q}$ and $\tilde{\mathbf{P}} = \Lambda_P \mathbf{P}$, and for the position vector $\tilde{\mathbf{r}} = \Lambda_r \mathbf{r}$, where Λ_i are nonzero scaling parameters. Taking this freedom into account we introduce the reduced quantities F (f_{tot}), \mathbf{Q} (equivalently S, x_0, r_1, r_2), \mathbf{P} (equivalently p_1, v_0), $\mathbf{r}, \mathbf{k}, t_Q, \rho_{2,2} - \rho_{4,16}, t_P, a_d, e_P, \lambda, c_b, d_b$ and e_b with the help of equations

$$\begin{aligned}
\tilde{F} &= \frac{b^2}{f} F \quad (\tilde{f}_{tot} = \frac{b^2}{f} f_{tot}), \quad \tilde{\mathbf{r}} = \frac{\sqrt[6]{f} \sqrt{L_1^{(2)}}}{b^{2/3}} \mathbf{r}, \quad \tilde{\mathbf{Q}} = \sqrt[3]{\frac{b}{f}} \mathbf{Q}, \\
\tilde{\mathbf{P}} &= \sqrt[3]{\frac{b}{f}} \sqrt{\frac{L_1^{(2)}}{b_P}} \mathbf{P}, \quad a_Q = \sqrt[3]{\frac{b^4}{f}} t_Q, \quad a_P = \frac{b^{4/3} b_P t_P}{\sqrt[3]{f} L_1^{(2)}}, \\
L_2^{(2)} &= L_1^{(2)} \rho_{2,2}, \quad L_i^{(3)} = \sqrt[3]{\frac{f}{b}} L_1^{(2)} \rho_{3,i}, \quad L_i^{(4)} = \sqrt[3]{\left(\frac{f}{b}\right)^2} L_1^{(2)} \rho_{4,i} \\
\lambda_i &= L_1^{(2)} l_i, \quad l_2 = \frac{\rho_{3,2}}{2 \rho_{4,14}}, \quad l_3 = \frac{\rho_{3,3}}{2 \rho_{4,6}}, \quad l_4 = \frac{\rho_{3,4}}{2 \rho_{4,7}}, \\
A_4 &= \frac{\sqrt[3]{b^2 f} a_d b_P^2}{\left(L_1^{(2)}\right)^2}, \quad \varepsilon_P = \frac{b^{2/3} \sqrt{b_P} e_P}{\sqrt[6]{f}}, \quad \Lambda_{QP} = \frac{b b_P}{L_1^{(2)}} \lambda, \\
c &= \sqrt[3]{b^2 f} c_b, \quad d = \sqrt[3]{b f^2} d_b, \quad \tilde{\mathbf{k}} = \frac{b^{2/3}}{\sqrt[6]{f} \sqrt{L_1^{(2)}}} \mathbf{k}.
\end{aligned} \tag{22}$$

The remaining quantities (S, x_0, r_1, r_2) and (p_1, v_0) are connected with their tilted counterparts by the same relations as \mathbf{Q} with $\tilde{\mathbf{Q}}$ and \mathbf{P} with $\tilde{\mathbf{P}}$, respectively. In addition, the

definitions (19) now become reduced to

$$\begin{aligned}\rho_{3,2} &= \rho_{3,8} - \rho_{3,7}, & \rho_{3,3} &= 2(\rho_{3,7} + \rho_{3,8}) \\ \rho_{4,6} &= 4(\rho_{4,15} - \rho_{4,16}), & \rho_{4,14} &= \rho_{4,15} + \rho_{4,16}.\end{aligned}\quad (23)$$

Consequently, the generalized Landau-de Gennes free energy expansion in terms of reduced variables \mathbf{Q} and \mathbf{P} reads

$$F = \frac{1}{V} \int_V f_{tot} d^3\mathbf{r} = \frac{1}{V} \int_V (f_{b,Q} + f_{e,Q} + f_P + f_{QP}) d^3\mathbf{r}, \quad (24)$$

where

$$f_{Qb} = f_{Qb}[I_2, I_3] = t_Q I_2 - I_3 + c_b I_2^2 + d_b I_2 I_3 + e_b (I_2^3 - 6I_3^2) + I_3^2, \quad (25)$$

$$\begin{aligned}f_{Qel} &= (1 + \rho_{4,7} l_4^2) Q_{\alpha\beta,\gamma} Q_{\alpha\beta,\gamma} + (\rho_{2,2} + \rho_{4,14} l_2^2 + \rho_{4,6} l_3^2) Q_{\alpha\beta,\beta} Q_{\alpha\gamma,\gamma} + \\ &(\rho_{3,8} - \rho_{3,7}) Q_{\alpha\beta} Q_{\alpha\mu,\beta} Q_{\mu\nu,\nu} + 2(\rho_{3,8} + \rho_{3,7}) Q_{\alpha\beta} Q_{\alpha\mu,\mu} Q_{\beta\nu,\nu} + \\ &\rho_{3,4} Q_{\alpha\beta} Q_{\alpha\mu,\nu} Q_{\beta\mu,\nu} + \rho_{4,7} Q_{\alpha\beta} Q_{\gamma\beta} Q_{\alpha\mu,\nu} Q_{\gamma\mu,\nu} + \\ &4(\rho_{4,15} - \rho_{4,16}) Q_{\alpha\beta} Q_{\gamma\beta} Q_{\alpha\mu,\mu} Q_{\gamma\nu,\nu} + (\rho_{4,15} + \rho_{4,16}) Q_{\alpha\beta} Q_{\gamma\delta} Q_{\alpha\mu,\beta} Q_{\gamma\mu,\delta},\end{aligned}\quad (26)$$

$$f_P = t_P \mathbf{P}^2 + a_d (\mathbf{P}^2)^2 + (\nabla \otimes \mathbf{P})^2, \quad (27)$$

$$f_{QP} = -e_P \mathbf{P} \cdot (\nabla \cdot \mathbf{Q}) - \lambda P_\alpha Q_{\alpha\beta} P_\beta, \quad (28)$$

and where $I_2 = \text{Tr}(\mathbf{Q}^2)$ and $I_3 = \text{Tr}(\mathbf{Q}^3)$. In this parameterization terms proportional to $\rho_{3,8}$ and $\rho_{4,16}$ vanish for UDS.

The expansion (24-28) is our GLdeG theory of modulated nematics. If we limit ourselves to a family of periodic structures with periodicity being developed in one spatial direction the nonzero cubic and quartic couplings: $\rho_{3,4}$, $\rho_{3,7}$, $\rho_{4,7}$ and $\rho_{4,15}$ should admit the UDS states as global minimizers. The remaining two couplings: $\rho_{3,8}$ and $\rho_{4,16}$ are solely responsible for one-dimensional, *nonuniform* periodic distortions, which makes the corresponding elastic terms vanish for UDS. This means that depending on the choice of $\rho_{3,8}$ and $\rho_{4,16}$ we should be able to eliminate inhomogeneously deformed structures from the ground states of GLdeG, leaving only UDS. In the remaining part of this paper we are going to concentrate exclusively on this simpler case.

V. BIFURCATION SCENARIOS FOR UNIFORMLY DEFORMED STRUCTURES

Here we limit ourselves to the UDS structures given in Table I and determine bifurcation conditions for various symmetry breaking transitions. Clearly, the isotropic-uniaxial

nematic bifurcation temperature is given by T^* (12), which represents spinodal, while the $I - N_U$ phase transition takes place at T_{NI} , slightly above T^* . Likewise, T_P entering a_P , Eq. (20), is transition temperature for a hypothetical phase transition from the isotropic to ferroelectric phase ($\mathbf{P} \neq 0$), in the absence of the nematic order ($\mathbf{Q} = 0$). Both, T^* and T_P are examples of bifurcation temperatures from less ordered phase (isotropic) - to more ordered one (nematic, ferroelectric). There are further bifurcations possible for UDS. Below, we give bifurcation conditions for all possible phase transitions between UDS given in Table I. The procedure is found in [12] and we only briefly sketch it below. For given material parameters the equilibrium amplitudes $y_i \in \{ r_1, r_2, p_1, x_0, v_0 \}$ are found from the minimization of the free energy F , Eq. (13), calculated for UDS (explicit formula for F is listed in the Supplementary Material). They are solutions of a system of polynomial equations $\psi_i(t_Q, t_P, \{y_\alpha\}) \equiv \partial F / \partial y_i = 0$. In order to employ a bifurcation analysis to $\{\psi_\alpha\}$ we expand y_i , t_Q and t_P in an arbitrary parameter ε :

$$\begin{aligned} y_i &= y_{i,0} + \varepsilon y_{i,1} + \varepsilon^2 y_{i,2} + \dots \\ t_m &= t_{m,0} + \varepsilon t_{m,1} + \varepsilon^2 t_{m,2} + \dots \quad m = Q, P, \end{aligned} \quad (29)$$

where non-vanishing $y_{i,0}$ define the reference, higher symmetric phase. For example, if the reference state is the N_U phase, only $y_{4,0} \equiv x_{0,0}$ is nonzero in Eqs. (29). By substituting Eqs. (29) into $\{\psi_\alpha = 0\}$ and letting equations of the same order in ε vanish we find equations for $y_{i,\alpha}$ and t_m , ($m = Q, P$). The leading terms, proportional to ε^0 , are equations describing the high-symmetric reference state. Terms of the order ε^1 give conditions for bifurcation to a low-symmetric phase. An equivalent approach would be to construct from F the effective Landau expansion $\delta f(y_p)$ in a primary order parameter y_p of low-symmetric phase by systematically eliminating the remaining parameters $\{y_i\}$. A detailed procedure is given in Ref. [29]. For example, in case of the $N_U - N_{TB}$ phase transition we could take for the primary order parameter either $y_1 \equiv r_1$ or $y_3 \equiv p_1$ with the final formulas being insensitive to the choice. Before we start it proves convenient to introduce auxiliary variables κ_1 and κ_2 :

$$\begin{aligned} \kappa_1 &= 1 + l_4^2 \rho_{4,7}, \\ \kappa_2 &= 2 \kappa_1 + \rho_{2,2} + l_2^2 \rho_{4,14} + l_3^2 \rho_{4,6}, \end{aligned} \quad (30)$$

and relative phases χ_1, χ_2 :

$$\begin{aligned}\chi_1 &= \phi_1 - \phi_p, \\ \chi_2 &= \phi_2 - 2\phi_p,\end{aligned}\tag{31}$$

which simplify the free energy and consequently also bifurcation formulas.

A. $I - N_{\text{TB}}$

A bifurcation condition for a phase transition from the isotropic phase to the nematic twist-bend phase can be written down as an equation connecting t_P and t_Q :

$$a \equiv a(t_P, t_Q) = 2(k^2 + t_P) - \frac{e_P^2 k^2 \sin^2(\chi_1)}{2\kappa_2 k^2 + 4t_Q} = 0.\tag{32}$$

If we permit the k -vector and χ_1 to vary, then the bifurcation temperature $t_{P,I-TB}$ from the isotropic to nematic twist-bend phases will be the maximal t_P fulfilling the condition (32). Solving Eq. (32) for t_P and maximizing with respect to k and χ gives the bifurcation values for k , $\sin(\chi_1)$ and t_P . They read

$$\begin{aligned}k_{I-TB}^2 &= \max\left(0, \frac{\sqrt{t_Q}|e_P|}{\sqrt{2}|\kappa_2|} - \frac{2t_Q}{\kappa_2}\right), \quad \text{for } t_Q > t_{NI} > 0, \quad \kappa_2 > 0 \\ \sin(\chi_{1,I-TB})^2 &= 1 \\ t_{P,I-TB} &= \begin{cases} 0 & \text{for } k_{I-TB} = 0 \\ \frac{e_P^2 + 8t_Q - 4\sqrt{2}\sqrt{t_Q}|e_P|}{4\kappa_2} & \text{for } k_{I-TB} > 0 \end{cases}\end{aligned}\tag{33}$$

where $t_{NI} > 0$ is the isotropic-uniaxial nematic transition temperature. Using formalism of Ref. [29] one can also show that the a -term, Eq. (32), is actually the leading coefficient in the Landau expansion of the free energy of the N_{TB} phase about the reference I phase in the primary order parameter p_1 :

$$\Delta f_{I-TB} = \frac{1}{2!} a p_1^2 + \frac{1}{4!} b p_1^4 + \frac{1}{6!} c p_1^6 + \dots\tag{34}$$

Generally, nonzero value k_{I-TB} of the k -vector at the bifurcation point ($e_P^2 > 8t_Q$) indicates that the $I - N_{\text{TB}}$ phase transition is, at least weakly, first order. It can be classified as an example of a weak crystallization introduced by Kats *et al.* [41], with fluctuations that should be observed near the $k = k_{I-TB}$ sphere. Interestingly, for $k = k_{I-TB} = 0$ a direct inspection of higher-order terms of the expansion (34) shows that $b = 24 a_d - \frac{\lambda^2}{t_Q}$ can change sign for sufficiently large λ . That is, for $c > 0$ the $I - N_{\text{TB}}$ transition can be first order ($a = 0, b < 0$), second order ($a = 0, b > 0$), or tricritical ($a = 0, b = 0$).

B. $N_U - N_{TB}$

A bifurcation condition from N_U to N_{TB} , expressed in terms of an equation connecting t_P and x_0 reads:

$$a \equiv a(t_P, x_0) = 2 \left(k^2 + t_P + \frac{\lambda x_0}{\sqrt{6}} \right) - \frac{3 e_P^2 \sin^2(\chi_1)}{6 \kappa_2 + x_0 (\sqrt{6} \kappa_3 + \kappa_4 x_0)} = 0 \quad (35)$$

where $\kappa_3 = \rho_{3,4} - 4\rho_{3,7}$, $\kappa_4 = 5\rho_{4,7} + 8\rho_{4,15}$ and where x_0 is the nematic order parameter calculated from the minimization of f_{Qb} in the uniaxial nematic phase. For fixed t_Q (x_0) the bifurcation temperature corresponds to the maximal t_P fulfilling the condition of $a = 0$, Eq. (35), where maximum is taken over k and χ_1 . It yields

$$t_{P,N-TB} = -\frac{\lambda x_0}{\sqrt{6}} + \frac{3e_P^2}{2(6\kappa_2 + \sqrt{6}\kappa_3 x_0 + \kappa_4 x_0^2)} \quad (36)$$

for $k = 0$ and $\sin^2(\chi_1) = 1$. As previously for the $I - N_{TB}$ phase transition, the a -term, Eq. (35), is the leading coefficient in Landau expansion of the free energy of the N_{TB} phase about the reference N_U phase in the primary order parameter p_1 [29]: $\Delta f_{N-TB} = \frac{1}{2!} a p_1^2 + \frac{1}{4!} b p_1^4 + \frac{1}{6!} c p_1^6 + \dots$. A direct inspection of this expansion shows that the $N_U - N_{TB}$ transition can be first order ($a = 0, b < 0, c > 0$), second order ($a = 0, b > 0, c > 0$), or tricritical ($a = 0, b = 0, c > 0$). Our analysis in the next section shows that for the case of CB7CB the predicted $N_U - N_{TB}$ transition is weakly first-order. The tricritical conditions for $I - N_{TB}$ and $N_U - N_{TB}$ phase transitions will be studied in detail elsewhere.

C. Bifurcations to globally polar phases

In a similar way we can derive the bifurcation condition for phase transitions from I , N_U , N_{TB} to corresponding globally polar structures listed in Table I. It reads

$$a = 2 t_P - 2\sqrt{\frac{2}{3}} \lambda x_0 + 4a_d p_1^2 = 0, \quad (37)$$

where $x_0 = p_1 = 0$ for $I - N_{U,p}$ bifurcation, $p_1 = 0$ for $N_U - N_{U,p}$ bifurcation, and where both x_0 and p_1 are non-zero when bifurcation takes place from N_{TB} to $N_{TB,p}$. Now the parameter a is the leading coefficient of Landau expansion $\Delta f_p = \frac{1}{2!} a v_0^2 + \frac{1}{4!} b v_0^4 + \frac{1}{6!} c v_0^6 + \dots$ in v_0 - the primary order parameter for phase transitions to polar structures. Given the form of the expansion for f_P , Eq. (20), the tricritical point can only be found for the $N_{TB} - N_{TB,p}$ phase transition.

VI. ESTIMATES OF MODEL PARAMETERS FROM EXPERIMENTAL DATA FOR CB7CB

Before we explore relative stability of the nematic phases given in Table I we estimate some of the material parameters entering the expansion (10) from experimental data in the uniaxial nematic phase. This will allow us to study properties of N_{TB} with only a few adjustable parameters. Indeed, nearly all of the parameters of the purely nematic parts: the bulk \tilde{f}_{Qb} and the elastic \tilde{f}_{Qel} can be correlated with the existing data in the uniaxial nematic phase. The N_{U} phase usually appears stable at higher temperatures and $N_{\text{U}} - N_{\text{TB}}$ phase transition is observed as temperature is lowered.

The very first compound shown to exhibit stable nematic and twist-bend nematic phase was the liquid crystal dimer 1'',7''-bis(4-cyanobiphenyl-4'-yl)heptane, abbreviated as CB7CB [5–7]. This compound is constituted of two 4-cyanobiphenyls (CB) linked by an alkylene spacer (C_7H_{14}). Currently, it is one of the best studied examples. In particular, Babakhanova *et al.* [20] have carried out a series of experiments for this mesogen in the uniaxial nematic phase. They determined the temperature variation of the nematic order parameter \tilde{S} (see Eq. (1)), the temperature variation of the Frank elastic constants K_{ii} ($i = 1, 2, 3$), the nematic-isotropic transition temperature T_{NI} , the nematic twist-bend-nematic transition temperature $T_{N_{\text{TB}}}$. We use the data presented in Table II to estimate some of the parameters of the extended LdeG theory.

A. Bulk part

Under the assumption that $\tilde{\mathbf{Q}}$ is uniaxial and positionally independent (Eq. 1 with $\hat{\mathbf{n}}(\tilde{\mathbf{r}}) = \text{const.}$), the order parameter \tilde{S} can be determined from the minimum of the free-energy density \tilde{f}_{Qb} , Eq. 11, which becomes reduced to that of the uniaxial nematic phase

$$\tilde{f}_{Qb} = \frac{2}{3}a_0Q(\Delta t + \Delta t_{NI})\tilde{S}^2 - \frac{2}{9}b\tilde{S}^3 + \frac{4}{9}c\tilde{S}^4 + \frac{4}{27}d\tilde{S}^5 + \frac{4}{81}f\tilde{S}^6. \quad (38)$$

Now, from the necessary condition for minimum, $\partial\tilde{f}_{Qb}/\partial\tilde{S} = 0$, solved for $T(\tilde{S})$, we determine the ratios $b/a_0 = \tilde{b}$, $c/a_0 = \tilde{c}$, $d/a_0 = \tilde{d}$ and $f/a_0 = \tilde{f}$ by fitting $\{\tilde{S}, T(\tilde{S})\}$ to the experimental data of Babakhanova *et al.* [20]. Independently, the scaling factor a_0 can be estimated from the latent heat per mole $\Delta H_{NI} = T_{NI} \left(\partial\tilde{f}_{Qb}/\partial T \right)_{T \rightarrow T_{NI}^-}$ for the nematic–isotropic phase

transition. It reads

$$a_0 = \frac{a_{0Q}}{T_{NI}} = \frac{3\Delta H_{NI}(2\tilde{S}_{NI}(24\tilde{c} + \tilde{S}_{NI}(15\tilde{d} + 8\tilde{f}\tilde{S}_{NI})) - 9\tilde{b})}{2\tilde{S}_{NI}T_{NI} \left(9\tilde{b}\tilde{S}_{NI} + 10\tilde{d}\tilde{S}_{NI}^3 + 8\tilde{f}\tilde{S}_{NI}^4 - 36T_{NI} + 36T^* \right)}, \quad (39)$$

where \tilde{S}_{NI} is the nematic order parameter at the uniaxial nematic–isotropic phase transition. For overall consistency, a_0 has been onward multiplied by $\rho_C = \rho/M_w \approx 2.22 * 10^3 \text{ mol/m}^3$, which is the ratio of the mass density ($\rho \approx 10^3 \text{ kg/m}^3$) to the relative molecular weight of CB7CB ($M_w \approx 0.45 \text{ kg/mol}$) yielding the value $6.88 \cdot 10^4 \text{ J m}^{-3} \text{ K}^{-1}$. Thanks to this operation it was possible to express all expansion coefficients in units J/m^{-3} . Fig. 3 depicts results of fitting to experimental data, whereas numerical values of the parameters are gathered in Table III. Please observe that the expansion parameter e couples to a purely biaxial part and therefore it cannot be estimated from the data in N_U .

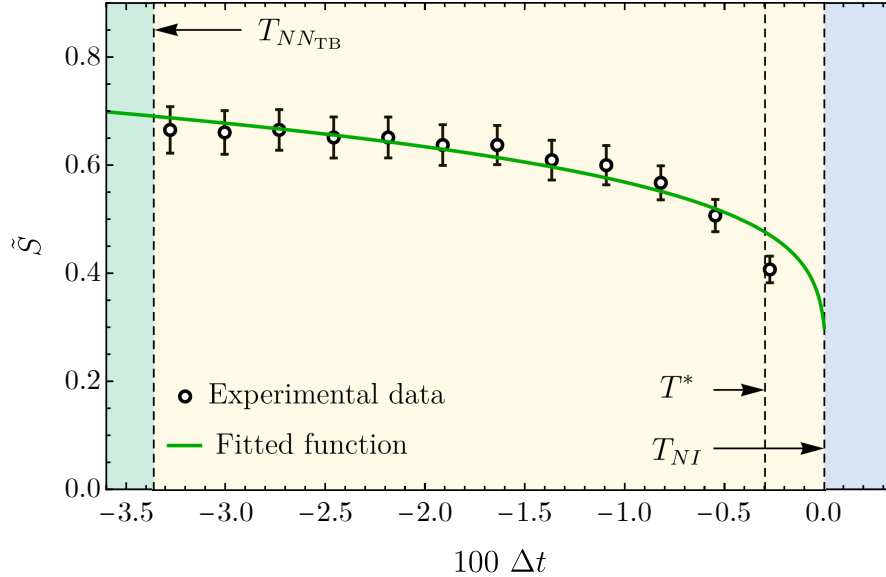


FIG. 3. Experimental data from [20] representing the temperature dependence of \tilde{S} in the uniaxial nematic phase of CB7CB. Green line illustrates the effect of fitting predictions of theory (38) to the data. T^* represents the maximal supercooling temperature of the isotropic phase. Our fit is carried out by taking as *ansatz* the experimentally known value of T_{NI} and T^* . Then \tilde{S}_{NI} for CB7CB is estimated from our fitted function. If we compromise the agreement of T_{NI} and T^* with experimental data a better fit can be obtained for \tilde{S} close to the transition temperature without affecting one in the vicinity of $N_U - N_{TB}$.

TABLE II. Basic experimental data for CB7CB used to estimate some of the parameters of the extended LdeG theory, along with other crucial data based on aforementioned estimates.

Nematic				
Description	Parameter	Value	Unit	Source
Temperature of nematic-isotropic phase transition	T_{NI}	387.15	K	[20]
Supercooling temperature of the isotropic phase	T^*	386	K	acquired from $\tilde{S}(T)$
Enthalpy	ΔH_{NI}	0.72	kJ/mol	[42]
Order parameter at T_{NI}	\tilde{S}_{NI}	0.3	-	acquired from $\tilde{S}(T = T_{NI})$
Twist-bend nematic				
Description	Parameter	Value	Unit	Source
Temperature of nematic-twist-bend nematic phase transition	$T_{NN_{TB}}$	374.15	K	[20]
Enthalpy	$\Delta H_{NN_{TB}}$	0.82	kJ/mol	[42]

Twist-bend nematic phase can be supercooled to about 304.15 K [5] and then there is a glass transition at approximately 277.15 K [43].

B. Flexopolarization renormalized elasticity of uniaxial nematics

It is important to realize that although (flexo)polarization terms (20,21) vanish in the uniaxial nematic phase any local deformation of the alignment tensor induces deformation of $\tilde{\mathbf{P}}$ due to the flexopolarization coupling $\varepsilon_P \neq 0$. Such deformations effectively renormalize elastic constants $L_m^{(n)}$ in ordinary nematic phases. The effect cannot be neglected if we intend to estimate $L_m^{(n)}$ from experimental data. A mathematical procedure of taking into account such deformations in the N_U phase is to minimize the free energy Eq. (10) over Fourier modes of the polarization field for given, fixed Fourier modes of the alignment tensor. Assuming that deformation $\tilde{\mathbf{Q}}(\tilde{\mathbf{r}})$ is small and slowly varying we obtain with this procedure the $\tilde{\mathbf{Q}}$ -

induced deformation of $\tilde{\mathbf{P}}(\tilde{\mathbf{r}})$ expressed in terms of Fourier modes which, when transformed back to the real space take the form of a series in $Q_{\alpha\mu}$, $Q_{\alpha\mu,\mu}$ and in higher-order derivatives of $Q_{\alpha\mu}$. The relevant terms are

$$\tilde{P}_\alpha(\tilde{\mathbf{r}}) = \frac{\varepsilon_P}{2a_P} \tilde{Q}_{\alpha\mu,\mu} + \frac{\varepsilon_P \Lambda_{QP}}{2a_P^2} \tilde{Q}_{\alpha\beta} \tilde{Q}_{\beta\mu,\mu} + \frac{\varepsilon_P \Lambda_{QP}^2}{2a_P^3} \tilde{Q}_{\alpha\lambda} \tilde{Q}_{\lambda\beta} \tilde{Q}_{\beta\mu,\mu} + \dots \quad (40)$$

Substituting Eq. (40) back to \tilde{f}_P and \tilde{f}_{QP} we obtain effective elastic contributions expressed in terms of only $\tilde{Q}_{\alpha\beta}$ and $\tilde{Q}_{\gamma\mu,\mu}$. When added to \tilde{f}_{Qel} they give an effective elastic free energy of uniaxial and biaxial nematics with $L_m^{(n)}$ being replaced by $L_{m,eff}^{(n)}$, where relevant $L_m^{(n)}$'s are

$$\begin{aligned} L_2^{(2)} &\rightarrow L_{2,eff}^{(2)} = L_2^{(2)} - \frac{\varepsilon_P^2}{4a_P}, \\ L_3^{(3)} &\rightarrow L_{3,eff}^{(3)} = L_3^{(3)} - \frac{\Lambda_{QP} \varepsilon_P^2}{4a_P^2}, \\ L_6^{(4)} &\rightarrow L_{6,eff}^{(4)} = L_6^{(4)} - \frac{\Lambda_{QP}^2 \varepsilon_P^2}{4a_P^3}. \end{aligned} \quad (41)$$

An important physical distinction between the bare constant $L_m^{(n)}$ and the renormalized constant $L_{m,eff}^{(n)}$ is of the same sort as one between renormalized and bare Frank elastic constants, as discussed by Jákli, Lavrentovich and Selinger [3]: $L_m^{(n)}$ gives the energy cost of $\tilde{Q}_{\alpha\beta,\gamma}$ deformations if we constrain $\tilde{P}_\alpha = 0$ during the deformation, while $L_{m,eff}^{(n)}$ relaxes to its optimum value during the the deformation. Assuming that major contribution to flexopolarization is of entropic, excluded volume type, any realistic experiment to measure elastic constants should not put constraints on the polar field $\tilde{\mathbf{P}}$, but rather allows it to relax. In this case, which is analysed here, $L_{m,eff}^{(n)}$ are the relevant contributions to the elastic constants in Eq. (14).

C. Elastic part

In the hydrodynamic limit where spatial dependence of \tilde{S} is disregarded and $\tilde{\mathbf{Q}}$ is given by (1) the elastic free energy \tilde{f}_{Qel} turns into the Oseen-Frank free energy density of the director field $\mathbf{n}(\tilde{\mathbf{r}})$, Eq. (2), with K_{11} , K_{22} and K_{33} being polynomials in \tilde{S} [28]

$$K_{ii} = K_{ii}^{(2)} \tilde{S}^2 + K_{ii}^{(3)} \tilde{S}^3 + K_{ii}^{(4)} \tilde{S}^4 \quad (i = 1, 2, 3). \quad (42)$$

The coefficients $K_{ii}^{(n)}$ are functions of $L_j^{(n)}$ [28, 30] fulfilling the splay-bend degeneracy relation in the second order: $K_{11}^{(2)} = K_{33}^{(2)}$. For completeness, they are given in Supplemental Material.

As it turns out $K_{ii}^{(n)}$ with $n = 2, 3, 4$ along with flexopolarization renormalization (41) are sufficient to obtain a good fit of Eq. (42) to experimentally observed K_{ii} for CB7CB [20]. Importantly, they also provide an estimate for the (flexo)polar couplings ε_P and Λ_{QP} . In finding $K_{ii}^{(n)}$ we use the $\tilde{S}(T)$ fit obtained from the analysis of the bulk free energy in Section (III A), which is a prerequisite to have a consistent theory of the uniaxial nematic phase for this compound. Results of fitting are gathered in Table III. Finally, as the number of relevant couplings $L_\alpha^{(n)}$ ($n = 3, 4$), Eq. (14), equals that of $K_{ii}^{(n)}$ we can correlate $L_\alpha^{(n)}$ with $K_{ii}^{(n)}$ using the results of Supplemental Material and of Ref. [28]. It yields

$$\begin{aligned}
L_1^{(2)} + \lambda_4^2 L_7^{(4)} &= \frac{1}{4} K_{22}^{(2)}, \\
L_2^{(2)} + \lambda_2^2 L_{14}^{(4)} + \lambda_3^2 L_6^{(4)} - \frac{\varepsilon_P^2}{4 a_P} &= \frac{1}{2} \left(K_{11}^{(2)} - K_{22}^{(2)} \right), \\
L_2^{(3)} &= \frac{1}{2} \left(K_{11}^{(3)} - 3K_{22}^{(3)} + 2K_{33}^{(3)} \right), \\
L_3^{(3)} - \frac{\Lambda_{QP} \varepsilon_P^2}{4 a_P^2} &= \frac{1}{2} \left(2K_{11}^{(3)} - 3K_{22}^{(3)} + K_{33}^{(3)} \right), \\
L_4^{(3)} &= \frac{3}{2} K_{22}^{(3)}, \\
L_6^{(4)} - \frac{\Lambda_{QP}^2 \varepsilon_P^2}{4 a_P^3} &= \frac{3}{10} \left(4K_{11}^{(4)} - 3K_{22}^{(4)} - K_{33}^{(4)} \right), \\
L_7^{(4)} &= \frac{9}{10} K_{22}^{(4)}, \\
L_{14}^{(4)} &= -\frac{3}{10} \left(K_{11}^{(4)} + 3K_{22}^{(4)} - 4K_{33}^{(4)} \right).
\end{aligned} \tag{43}$$

Results of fitting of $L_\alpha^{(n)}$, Eq. (14), obeying stability ansatz (15) to experimental data for CB7CB are given in Table III. Quality of fit is displayed in Fig. 4.

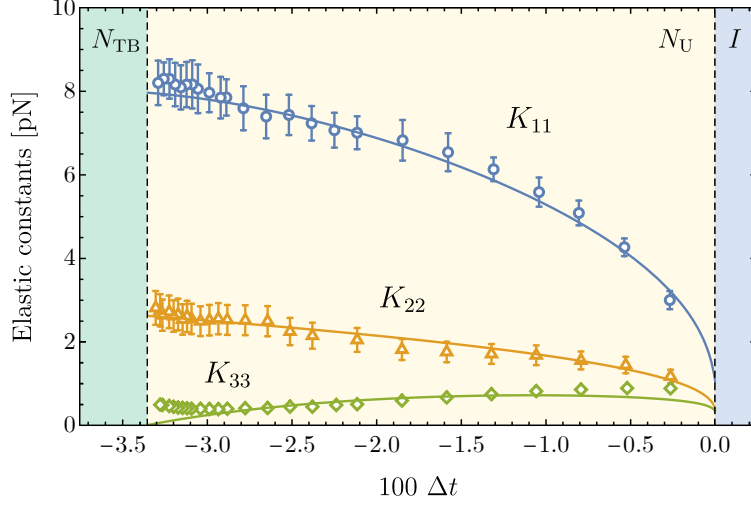


FIG. 4. Temperature dependence of elastic constants acquired from [20]. Continuous lines depict adopted approach for elastic constants within the model. Note that the model cannot explain a slight increase of K_{33} in the vicinity of the $N_U - N_{TB}$ phase transition.

TABLE III. Values of fitted coefficients of the bulk (38) and elastic constants (42) expansions, along with ones resulting from the flexopolarization renormalization. Additionally, according to (14) and (43) are provided $K_{ii}^{(n)}$ elastic constants.

Coefficient	Value [$\times 10^7$ J/m ³]	Coefficient	Value [pN]	Coefficient	Value [pN]
a_{0Q}	2.66	$K_{11}^{(2)} = K_{33}^{(2)}$	3.54	$L_1^{(2)}$	0.93
b	0.27	$K_{22}^{(2)}$	3.72	$L_2^{(2)}$	-0.0045
c	0.60	$K_{11}^{(3)}$	11.08	$L_2^{(3)}$	-11.16
d	-3.80	$K_{22}^{(3)}$	0.60	$L_3^{(3)}$	2.27
f	9.64	$K_{33}^{(3)}$	-15.80	$L_4^{(3)}$	0.90
		$K_{11}^{(4)}$	9.93	$L_6^{(4)}$	6.29
		$K_{22}^{(4)}$	1.77	$L_7^{(4)}$	1.59
		$K_{33}^{(4)}$	13.45	$L_{14}^{(4)}$	11.56
				$\frac{\varepsilon_P^2}{4a_P}$	0.08
				$\frac{\Lambda_{QP}\varepsilon_P^2}{4a_P^2}$	0.00013

$$T_P = 362 \text{ K}$$

VII. PREDICTIONS FOR NEMATIC TWIST-BEND PHASE OF CB7CB-LIKE COMPOUNDS

Within this section, we explore the relative stability of the UDS structures, listed in Table I, for the model Eq. (24) with parameters (estimated in previous sections), which are gathered in Table IV. We limit ourselves to the temperature interval where the N_{TB} phase appears stable in the experiment (Table V).

TABLE IV. Dimensionless parameters related to bulk part, elastic constants and bifurcation equations. Below are provided converters for $\Delta t \leftrightarrow t_Q$, $\tilde{\mathbf{r}} \leftrightarrow \mathbf{r}$ and $\tilde{\mathbf{k}} \leftrightarrow \mathbf{k}$.

Parameter	Value	Parameter	Value	Parameter	Value
c_b	0.67	$\rho_{2,2}$	-0.0048	l_2	-1.58
d_b	-1.29	$\rho_{3,2}$	-3.64	l_3	0.59
Δt_{NI}	0.0029	$\rho_{3,3}$	0.74	l_4	0.93
		$\rho_{3,4}$	0.29	κ_1	1.13
		$\rho_{4,6}$	0.62	κ_2	5.38
		$\rho_{4,7}$	0.15	κ_3	-7.73
		$\rho_{4,14}$	1.14	κ_4	6.0054

$$t_Q = 32.36(\Delta t + \Delta t_{NI}) \quad \tilde{\mathbf{r}} [\text{nm}] = 1.06 \mathbf{r} \quad \tilde{\mathbf{k}} [\text{nm}^{-1}] = 0.94 \mathbf{k}$$

TABLE V. Temperature ranges in Δt and t_Q units for stable liquid crystalline structures: nematic and twist-bend nematic from experiment [20].

Range of temperature parameter	Description
$-0.03 < \Delta t \leq 0$	nematic
$\Delta t \leq -0.03$	twist-bend nematic
$-0.99 < t_Q \leq 0.09$	nematic
$t_Q \leq -0.99$	twist-bend nematic

The temperatures t_P and t_Q are connected with absolute temperature T of the system studied (see Eqs. (12,20,22)). Since $a_P > 0$, $a_Q > 0$, $T^* > T_P$ and $T > T_P$ any straight line in $\{t_Q, t_P\}$ plane with positive slope and negative t_Q -intercept represents a permissible

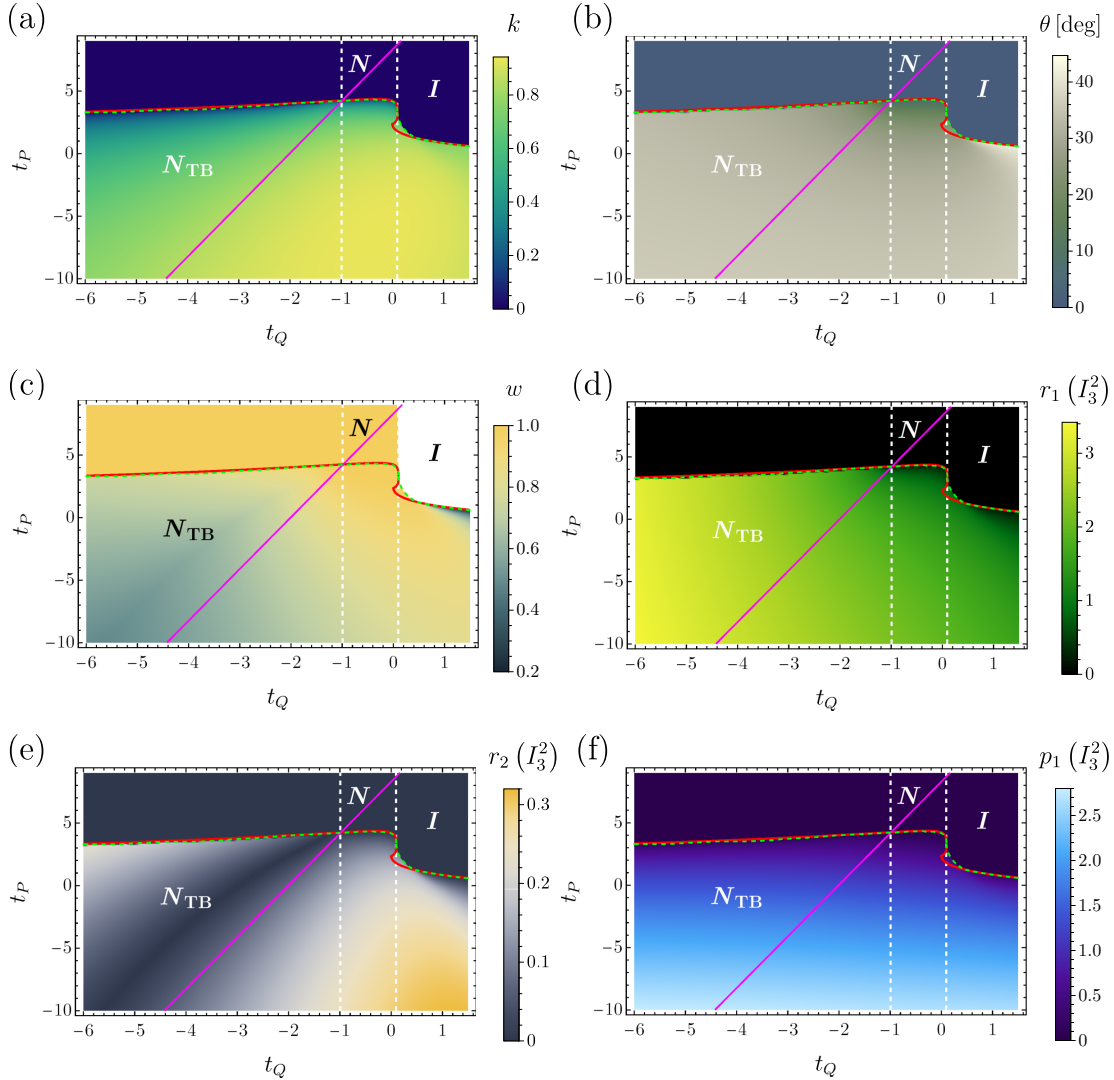


FIG. 5. Phase diagram combined with density map of wave vector k (a), tilt angle θ (b), biaxiality parameter w (c) and mode's amplitudes: r_1 (d), r_2 (e) and p_1 (f) within theory (I_3^2). Red continuous curve marks the bifurcation between $N \leftrightarrow N_{TB}$ and $I \leftrightarrow N_{TB}$, whereas dashed green curve outlines the numerical results. Magenta line (described by Eq. (44)) reflects the phase sequence associated directly with the experimental data for CB7CB. Vertical, dashed white lines designate the temperature span of N_U stability (experimental) mapped on t_Q (see Table V).

physical system with no polar order for $\tilde{\mathbf{Q}} = 0$. Thus, we present the phase diagrams in the general $\{t_Q, t_P\}$ plane for a broader view. In our case, the experimental-related line has the form:

$$t_P = 4.13t_Q + 8.29. \quad (44)$$

Results of our in-depth analysis, profoundly reduced the number of adjustable parameters for CB7CB-like compounds to solely four (λ , e_P , a_d , and e_b). From considerations related to the elastic constants, Table III, it turns out that Λ_{QP} (*ipso facto* λ), responsible for globally polar structures, is negligible, i.e. $\sqrt{|\lambda|}/e_P \approx 10^{-13}$. Thus, we set $\lambda = 0$. Onward, we take $e_P = 7.1$ and $a_d = 0.75$ as the best values to reproduce the temperature dependance of k . For the bulk biaxial parameter e_b we take two values: $e_b = 0$ and $e_b = 1/6$. If we recall Eq. (25), there is a term $e_b(I_2^3 - 6I_3^2) + I_3^2$. If we set $e_b = 0$, then it reduces to I_3^2 , on the other hand when we set $e_b = 1/6$ then we have only $I_2^3/6$. In the following discussion the first scenario ($e_b = 0$) will be referred to as theory (I_3^2) and second one as theory (I_2^3). The (I_3^2) theory will enhance phase biaxiality due to its tendency to lower equilibrium value of the w parameter, Eq. (9), while the (I_2^3) theory is promoting the $w = \pm 1$ states through cubic and fifth-order terms in (25) [32]. In this latter case the biaxiality of N_{TB} can only be induced by the elastic terms.

Figs. 5a-f depict phase diagrams combined with density maps of k , θ , w , r_1 , r_2 and p_1 , respectively, which are outcomes of theory (I_3^2). In the analyzed case, being consistent with the experiment, stable, apart from isotropic, is the uniaxial nematic phase and the twist-bend nematic phase. Dashed green curve denotes numerically determined phase transitions and red continuous curve marks the results from the bifurcation analysis (*see* Section V). Vertical, dashed white lines designate the temperature span of N_U stability (experimental) mapped on t_Q (*see* Table V). The purple straight line described by the Eq. (44) represents phase transition sequence: $I \leftrightarrow N_U \leftrightarrow N_{TB}$ based on the CB7CB data from [20]. From points lying on this line we have attained information about the behavior of pitch (p), tilt angle (θ) and nematic order parameter (\tilde{S}) in N_{TB} , alongside the insight into the N_{TB} 's biaxiality parameter (w) and the remaining order parameters (r_1 , r_2 , p_1) (*see* Figs. 6a-e). With regard to the w parameter, in the literature there are not available any results concerning the biaxiality of N_{TB} , thus it is hard to compare. Nevertheless, our model permits to estimate the span and magnitude of affect on experimentally measurable parameters.

We set together results of our model with available experimental data concerning pitch p (Fig. 6a [7, 44]), tilt angle θ (Fig. 6b [45–50]) and nematic order parameter \tilde{S} (Fig. 6c [20, 49–51]). At the transition temperature from N_U to N_{TB} the pitch length is ca. 54 nm and with decreasing temperature it saturates at the level of ca. 8 nm (Fig. 6a). As one can see, it goes fairly well with the experimental data. Within the literature the methodology

regarding the pitch measurements for CB7CB are consistent, i.e. all indicate that the pitch value reaches the plateau at ca. 8 nm [6, 7, 44], in contradiction to measurements of θ and \tilde{S} .

Such span of experimental data for θ , Fig. 6b, originate from the adopted method of determination and sample treatment. In Refs. [45], [46] and [48] birefringence measurements were employed, however the choice of region in which they were taken varied across the aforementioned papers (*see discussion in* [46]). In Refs. [49] and [50] the data regarding the conical tilt angle were extracted from X-ray methods, wherein in Ref. [49] it was small/wide angle X-ray scattering (SAXS/WAXS) and in Ref. [50] X-ray diffraction (XRD). In turn, conical tilt angle from Ref. [47] was determined *i.a.* from ^2H Nuclear Magnetic Resonance (NMR) quadrupolar splittings of CB7CB- d_4 . Similarly to tilt angle, discrepancies between the data related to order parameter, Fig. 6c, arise from the method of acquisition. In Ref. [20] it was extracted from diamagnetic anisotropy measurements, in Ref. [49] from SAXS, in Ref. [50] from XRD and in Refs. [50, 51] from polarized Raman spectroscopy (PRS). As one can see data from Ref. [20] stands out from the rest of the data (Fig. 6c), although it was the only source that provided simultaneously the data for the temperature dependence of orientational order parameter and elastic constants.

One can see that results of our model are generally in a very good agreement with experimental results, perhaps except an immediate vicinity of the $N_U - N_{\text{TB}}$ phase transition where fluctuations - not included in the present analysis - may play a role. Interesting seem predictions concerning the effect of intrinsic, molecular biaxiality on N_{TB} . While pitch, \tilde{S} and p_1 are practically insensitive to w the remaining observables are affected. In particular, for tilt angle the green continuous line, associated with $e_b = 0$ fits well in between the data from Refs. [45] (blue circles) and [48] (yellow squares), whereas the red dashed line, associated with the weakly biaxial case, markedly departs from the above experimental data. Based on the results of Babakhankova *et al.* [20] we can conclude that biaxiality of N_{TB} , initially small at the $N_U - N_{\text{TB}}$ phase transition, considerably increases on departing from the transition temperature (green line in Fig. 6d). Fig. 6e illustrates the behavior of the order parameters r_1 , r_2 and p_1 in N_{TB} phase of CB7CB, where the ratio $\sigma = r_1/r_2$ can be correlated with data acquirable from resonant soft X-ray scattering (RSoXS) [44, 53, 54]. In order to make this correlation, we translated our formalism into the one presented in [52]. Thanks to that, we could tie the results for σ with experimentally measurable scattering

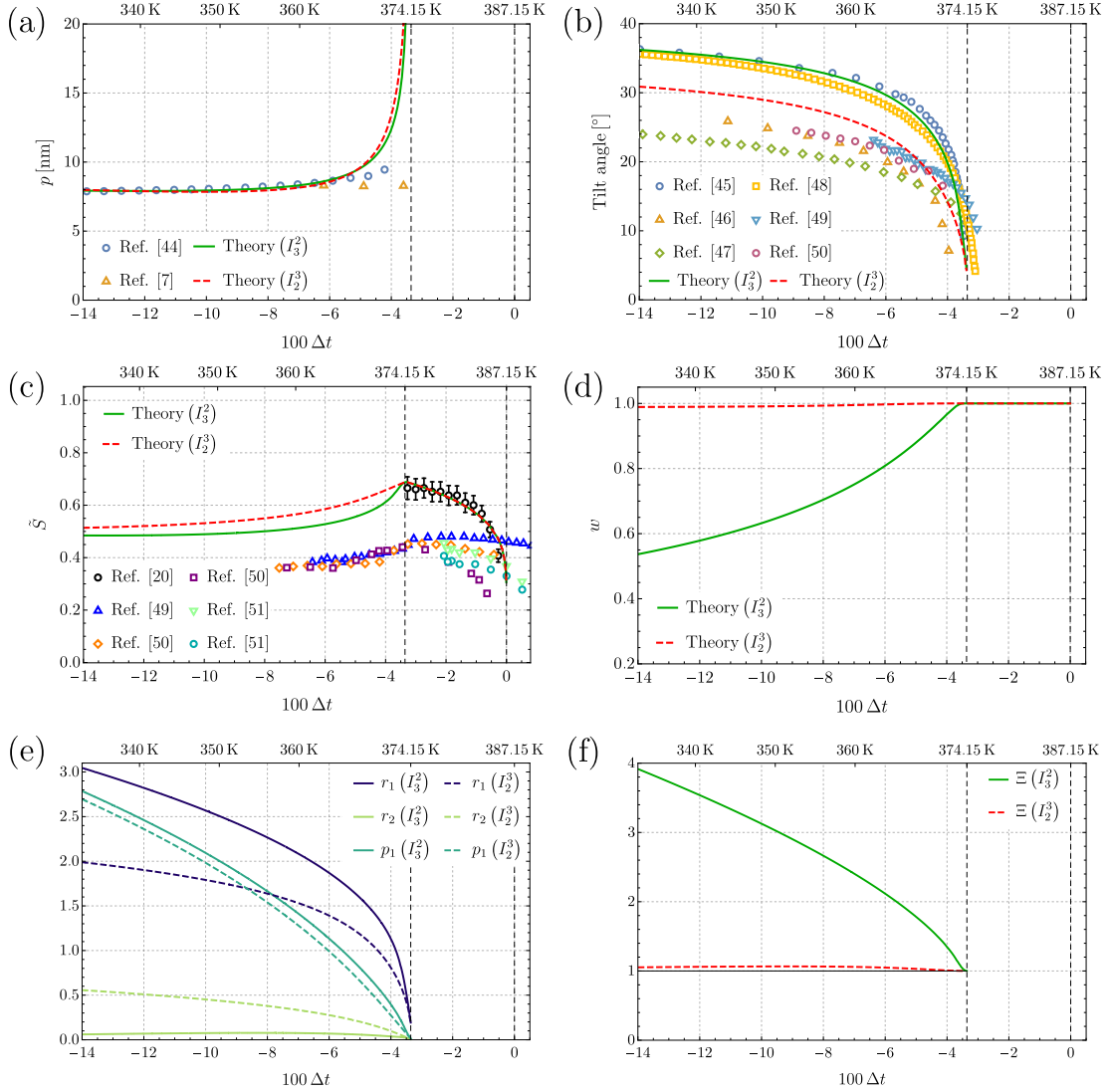


FIG. 6. Comparison between experimental data (hollow points) and theoretical predictions (continuous green and dashed red line) for CB7CB's N_{TB} 's temperature dependence of pitch p (a), tilt angle θ (b) and order parameter \tilde{S} (c). Plot (d) depicts the behaviour of biaxiality parameter w and plot (e) mode's amplitudes: r_1 , r_2 and p_1 as a function of temperature in the range of N_{TB} stability. Plot (f) illustrates the temperature behaviour of the relevant factor parameterizing the relative magnitudes of intensities of two leading harmonics of the dispersion tensor that contribute to the resonant soft X-ray scattering (RSoXS) [52]. All the data is drawn both with respect to the multiplied by factor 100 reduced temperature Δt , whereas key temperatures, corresponding to given Δt , are designated above each plot in absolute temperature T .

intensities through following formula:

$$\Xi = -\frac{1}{2} + \frac{3\sigma}{2\sigma \cos(2\theta) + 4 \sin(2\theta)}, \quad (45)$$

where $\Xi = f_1/f_2$ and θ is a conical tilt angle. The value of parameter Ξ determines the intensity of the $2q_0$ peak (half-pitch band) with the respect to the intensity of the q_0 peak (full pitch band) in the N_{TB} phase, where $q_0 = 2\pi/p$ is the magnitude of the wave vector of the heliconical deformation with the pitch p . As it was stated in [52], if $\Xi \geq 1$ then the intensity of the $2q_0$ peak is approximately two orders of magnitude lower than the intensity of the q_0 peak and further strongly decreases with increasing Ξ . On the other hand, if $\Xi < 1$ then the intensity of the $2q_0$ peak escalates rapidly. As one can see in Fig. 6f, which illustrates the temperature dependence of Ξ for both theories I_3^2 and I_2^3 , all the data obeys the relation $\Xi \geq 1$ indicating a significant weakness of $2q_0$ peak. Interestingly, while for the I_2^3 theory the relative magnitude of the intensities should roughly differ by two orders of magnitude irrespective of the temperature the I_3^2 model predicts further strong reduction of the relative intensity with temperature. To our best knowledge, the $2q_0$ signal has not been detected so far in any of the examined N_{TB} forming compounds [44, 53–55].

VIII. CONCLUSIONS

Currently existing experimental data are in favour of the theory that the $N_{\text{U}} - N_{\text{TB}}$ phase transition is driven by the flexopolarization mechanism. According to this theory deformations of the director induce local polar order which, in turn, renormalizes the bend elastic constant to a very small value relative to other elastic constants, eventually leading to the twist-bend instability. However, a fundamental description of orientational properties of nematics based on minimal coupling Landau-de Gennes theory of flexopolarization suggests that such behavior does not need to be universal. Even when both K_{11} and K_{33} are simultaneously reduced due to splay-bend degeneracy (inherent to the minimal coupling LdeG expansion) the N_{TB} phase can still become absolutely stable among all possible one dimensional periodic structures. Since this case has not been observed experimentally to date an important question that arises is whether the flexopolarization mechanism is indeed sufficient to explain the experimental observations at the level of the “first principles” Landau-deGennes theory of orientational order. In this work we gave a positive answer to

this question. We demonstrated that the experimental observations involving the nematic twist-bend phase and the related uniaxial nematic phase can be explained if we generalize the minimal coupling theory to the level where the properties of high-temperature uniaxial nematic phase are properly accounted for. Especially, the constructed generalized free energy density is in line with experimentally observed temperature variation of the Frank elastic constants and of the orientational order parameter.

Our proposed generalized theory of uniformly distorted nematics extends the elastic part of LdeG by additional two terms of third-order. The added elastic terms are the only independent ones for UDF and depending on model parameters various UDF structures can become minimizers of the free energy, including nematic twist-bend. This conclusion follows directly from the bifurcation analysis and from the observation that the remaining four independent elastic terms, not included in the theory, can always be written in such a way that they vanish for UDF. It is worth noticing that only one more term is generally needed to extend the studies of the UDF class to *all possible* one-dimensional distortions of the alignment tensor. This sort of classification of various elastic terms is similar to what Virga has recently proposed for generalized Frank's elastic theory [56].

The numerical analysis of the model quite well reproduces measured quantities for the N_U and N_{TB} phases of the CB7CB-like mesogens and gives numerical estimates for its constitutive parameters including otherwise difficult to access (flexo-)polarization couplings. Overall, the N_{TB} phase is predicted to be biaxial with theoretical support that major contribution to the phase biaxiality comes from bulk terms in the free energy. The phase transition to the N_{TB} is weakly first-order although, in general, the theory permits the transitions to N_{TB} be second order with tricritical $I - N_{TB}$ and $N_U - N_{TB}$ points.

Summarizing, the theory successfully links the chiral order of N_{TB} with the flexopolarization mechanism. It can also serve as a starting point in seeking for a new classes of modulated nematic structures, like nematic splay or nematic splay-bend ones.

ACKNOWLEDGMENTS

This work was partly supported by the Grant No. DEC-2013/11/B/ST3/04247 of the National Science Centre in Poland. LL acknowledges partial support by the EPSRC grant EP/R014604/1 [The Mathematical Design of New Materials-2019] of the Isaac Newton In-

stitute for Mathematical Sciences, University of Cambridge, UK. WT acknowledges a partial support by Marian Smoluchowski Scholarship (KNOW/58/SS/WT/2016) from Marian Smoluchowski Cracow Scientific Consortium “Matter-Energy-Future” within the KNOW grant and by Jagiellonian Interdisciplinary PhD Programme co-financed from the European Union funds under the European Social Fund (POWR.03.05.00-00-Z309/17-00). Results from this work were presented during the 2019 Gordon Conference on Liquid Crystals (July 7 - 12, New London, NH, USA) and the Erwin Schrödinger Institute (ESI) Workshop: New trends in the variational modeling and simulation of liquid crystals (December 2 - 6, Vienna, Austria, 2019).

-
- [1] P. G. de Gennes and J. Prost, *The Physics of Liquid Crystals*, 2nd ed. (Clarendon Press, 1993).
 - [2] H. Takezoe, E. Gorecka, and M. Čepič, *Rev. Mod. Phys.* **82**, 897 (2010).
 - [3] A. Jákli, O. D. Lavrentovich, and J. V. Selinger, *Rev. Mod. Phys.* **90**, 045004 (2018).
 - [4] V. P. Panov, M. Nagaraj, J. K. Vij, Y. P. Panarin, A. Kohlmeier, M. G. Tamba, R. A. Lewis, and G. H. Mehl, *Phys. Rev. Lett.* **105**, 167801 (2010).
 - [5] M. Cestari, S. Diez-Berart, D. A. Dunmur, A. Ferrarini, M. R. de La Fuente, D. J. B. Jackson, D. O. López, G. R. Luckhurst, M. A. Perez-Jubindo, R. M. Richardson, J. Salud, B. A. Timimi, and H. Zimmermann, *Phys. Rev. E* **84**, 031704 (2011).
 - [6] V. Borshch, Y.-K. Kim, J. Xiang, M. Gao, A. Jákli, V. P. Panov, J. K. Vij, C. T. Imrie, M. G. Tamba, G. H. Mehl, and O. D. Lavrentovich, *Nat. Commun.* **4**, 2635 (2013).
 - [7] D. Chen, J. H. Porada, J. B. Hooper, A. Klittnick, Y. Shen, M. R. Tuchband, E. Korblova, D. Bedrov, D. M. Walba, M. A. Glaser, J. E. MacLennan, and N. A. Clark, *Proc. Natl. Acad. Sci. USA* **110**, 15931 (2013).
 - [8] A. Mertelj, L. Cmok, N. Sebastián, R. J. Mandle, R. R. Parker, A. C. Whitwood, J. W. Goodby, and M. Čopič, *Phys. Rev. X* **8**, 041025 (2018).
 - [9] M. R. Tuchband, D. A. Paterson, M. Salamończyk, V. A. Norman, A. N. Scarbrough, E. Forsyth, E. Garcia, C. Wang, J. M. D. Storey, D. M. Walba, S. Sprunt, A. Jákli, C. Zhu, C. T. Imrie, and N. A. Clark, *Proc. Natl. Acad. Sci. USA* **116**, 10698 (2019).
 - [10] S. Srigengan, M. Nagaraj, A. Ferrarini, R. Mandle, S. J. Cowling, M. A. Osipov, G. Pająk, J. W. Goodby, and H. F. Gleeson, *J. Mater. Chem. C* **6**, 980 (2018).

- [11] G. Pająk, L. Longa, and A. Chrzanowska, Proc. Natl. Acad. Sci. U.S.A. **115**, E10303 (2018).
- [12] L. Longa and G. Pająk, Phys. Rev. E **93**, 040701 (2016).
- [13] C. T. Archbold, E. J. Davis, R. J. Mandle, S. J. Cowling, and J. W. Goodby, Soft Matter **11**, 7547 (2015).
- [14] A. A. Dawood, M. C. Grossel, G. R. Luckhurst, R. M. Richardson, B. A. Timimi, N. J. Wells, and Y. Z. Yousif, Liq. Cryst. **43**, 2 (2016).
- [15] R. B. Meyer, in *Proceedings of the Les Houches Summer School on Theoretical Physics, 1973, session No. XXV*, edited by R. Balian and G. Weill (Gordon and Breach Science Publishers, 1976) p. 271.
- [16] I. Dozov, Europhys. Lett. **56**, 247 (2001).
- [17] C. W. Oseen, Trans. Faraday Soc. **29**, 883 (1933).
- [18] F. C. Frank, Discuss. Faraday Soc. **25**, 19 (1958).
- [19] S. M. Shamid, S. Dhakal, and J. V. Selinger, Phys. Rev. E **87**, 052503 (2013).
- [20] G. Babakhanova, Z. Parsouzi, S. Paladugu, H. Wang, Y. A. Nastishin, S. V. Shiyanovskii, S. Sprunt, and O. D. Lavrentovich, Phys. Rev. E **96**, 062704 (2017).
- [21] G. Cukrov, Y. M. Golestani, J. Xiang, Y. A. Nastishin, Z. Ahmed, C. Welch, G. H. Mehl, and O. D. Lavrentovich, Liq. Cryst. **44**, 219 (2017).
- [22] K. L. Atkinson, S. M. Morris, F. Castles, M. M. Qasim, D. J. Gardiner, and H. J. Coles, Phys. Rev. E **85**, 012701 (2012).
- [23] E. C. Gartland Jr., Math. Model. Anal. **23**, 414 (2018).
- [24] L. Longa and H.-R. Trebin, Phys. Rev. A **42**, 3453 (1990).
- [25] K. Merkel, A. Kocot, J. K. Vijj, and G. Shanker, Phys. Rev. E **98**, 022704 (2018).
- [26] R. J. Mandle, E. J. Davis, C. T. Archbold, C. C. A. Voll, J. L. Andrews, S. J. Cowling, and J. W. Goodby, Chem. Eur. J. **21**, 8158 (2015).
- [27] D. W. Berreman and S. Meiboom, Phys. Rev. A **30**, 1955 (1984).
- [28] L. Longa, D. Monselesan, and H.-R. Trebin, Liq. Cryst. **2**, 769 (1987).
- [29] L. Longa, J. Chem. Phys. **85**, 2974 (1986).
- [30] L. Longa and H.-R. Trebin, Phys. Rev. A **39**, 2160 (1989).
- [31] L. Longa and W. Tomczyk, Liq. Cryst. **45**, 2074 (2018).
- [32] D. Allender and L. Longa, Phys. Rev. E **78**, 011704 (2008).
- [33] C. Greco and A. Ferrarini, Phys. Rev. Lett. **115**, 147801 (2015).

- [34] E. F. Gramsbergen, L. Longa, and W. H. de Jeu, *Phys. Rep.* **135**, 195 (1986).
- [35] L. Longa and G. Pająk, (2016), see Supplemental Material of [*Phys. Rev. E* **93**, 040701(R), 2016], which is available at: http://journals.aps.org/pre/supplemental/10.1103/PhysRevE.93.040701/Supplemental_material.pdf.
- [36] C. Greco, G. R. Luckhurst, and A. Ferrarini, *Soft Matter* **10**, 9318 (2014).
- [37] A. Ferrarini, *Liq. Cryst.* **44**, 45 (2017).
- [38] M. A. Osipov and G. Pająk, *Eur. Phys. J. E* **39**, 45 (2016).
- [39] W. Tomczyk, G. Pająk, and L. Longa, *Soft Matter* **12**, 7445 (2016).
- [40] W. Tomczyk and L. Longa, *Soft Matter* (2020), 10.1039/D0SM00078G.
- [41] E. Kats, V. Lebedev, and A. Muratov, *Phys. Rep.* **228**, 1 (1993).
- [42] D. A. Paterson, J. P. Abberley, W. T. Harrison, J. M. Storey, and C. T. Imrie, *Liq. Cryst.* **44**, 127 (2017).
- [43] D. O. López, N. Sebastian, M. R. de la Fuente, J. C. Martínez-García, J. Salud, M. A. Pérez-Jubindo, S. Diez-Berart, D. A. Dunmur, and G. R. Luckhurst, *J. Chem. Phys.* **137**, 034502 (2012).
- [44] C. Zhu, M. R. Tuchband, A. Young, M. Shuai, A. Scarbrough, D. M. Walba, J. E. MacLennan, C. Wang, A. Hexemer, and N. A. Clark, *Phys. Rev. Lett.* **116**, 147803 (2016).
- [45] C. Meyer, G. R. Luckhurst, and I. Dozov, *J. Mater. Chem. C* **3**, 318 (2015).
- [46] M. R. Tuchband, M. Shuai, K. A. Graber, D. Chen, C. Zhu, L. Radzihovsky, A. Klitnick, L. M. Foley, A. Scarbrough, J. H. Porada, M. Moran, J. Yelk, D. Bedrov, E. Korblova, D. M. Walba, A. Hexemer, J. E. MacLennan, M. A. Glaser, and N. A. Clark, “Double-Helical Tiled Chain Structure of the Twist-Bend Liquid Crystal phase in CB7CB,” (2017), arXiv:1703.10787 [cond-mat.soft].
- [47] J. P. Jokisaari, G. R. Luckhurst, B. A. Timimi, J. Zhu, and H. Zimmermann, *Liq. Cryst.* **42**, 708 (2015).
- [48] N. Vaupotič, M. Ali, P. W. Majewski, E. Gorecka, and D. Pociecha, *ChemPhysChem* **19**, 2566 (2018).
- [49] R. J. Mandle and J. W. Goodby, *Phys. Chem. Chem. Phys.* **21**, 6839 (2019).
- [50] G. Singh, J. Fu, D. M. Agra-Kooijman, J.-K. Song, M. R. Vengatesan, M. Srinivasarao, M. R. Fisch, and S. Kumar, *Phys. Rev. E* **94**, 060701 (2016).
- [51] Z. Zhang, V. P. Panov, M. Nagaraj, R. J. Mandle, J. W. Goodby, G. R. Luckhurst, J. C.

- Jones, and H. F. Gleeson, *J. Mater. Chem. C* **3**, 10007 (2015).
- [52] M. Salamończyk, N. Vaupotič, D. Pocięcha, C. Wang, C. Zhu, and E. Gorecka, (2017), see Supplemental Material of [*Soft Matter* **13**, 6694, 2017], which is available at: www.rsc.org/suppdata/c7/sm/c7sm00967d/c7sm00967d1.pdf.
- [53] M. Salamończyk, N. Vaupotič, D. Pocięcha, C. Wang, C. Zhu, and E. Gorecka, *Soft Matter* **13**, 6694 (2017).
- [54] M. Salamończyk, R. J. Mandle, A. Makal, A. Liebman-Peláez, J. Feng, J. W. Goodby, and C. Zhu, *Soft Matter* **14**, 9760 (2018).
- [55] W. D. Stevenson, Z. Ahmed, X. B. Zeng, C. Welch, G. Ungar, and G. H. Mehl, *Phys. Chem. Chem. Phys.* **19**, 13449 (2017).
- [56] E. G. Virga, *Phys. Rev. E* **100**, 052701 (2019).